Differences in the gut microbiomes of distinct ethnicities within the same geographic area are linked to host metabolic health

Qi Yan Ang[1,6], Diana L. Alba[2,3,6], Vaibhav Upadhyay[1,6], Jordan E. Bisanz[1], Jingwei Cai[4], Ho Lim Lee[2], Eliseo Barajas[2], Grace Wei[2], Andrew D. Patterson[4], Suneil K. Koliwad[2,3]*, and Peter J. Turnbaugh[1,5]*

[1]Department of Microbiology and Immunology, G.W. Hooper Research Foundation, University of California, San Francisco, CA 94143, USA

[2]Diabetes Center, University of California San Francisco, CA 94143, USA

[3]Division of Endocrinology, Diabetes, and Metabolism, Department of Medicine, University of California San Francisco, CA 94143, USA

[4]Center for Molecular Toxicology and Carcinogenesis, Department of Veterinary & Biomedical Sciences, Pennsylvania State University, PA 16802, USA

[5]Chan Zuckerberg Biohub, San Francisco, CA 94158, USA

[6]These authors contributed equally

*Correspondence to: Suneil K. Koliwad, M.D., Ph.D., Suneil.Koliwad@ucsf.edu, and Peter J. Turnbaugh, Ph.D., peter.turnbaugh@ucsf.edu

Author emails: qang@broadinstitute.org, vaibhav.upadhyay@ucsf.edu, diana.alba@ucsf.edu, jordan.bisanz@ucsf.edu, jingweicai313@gmail.com, adp117@psu.edu, holim.lee@wakehealth.edu, eliseojb2011@gmail.com

ABSTRACT

Background: The human gut microbiota exhibits marked variation around the world, which has been attributed to dietary intake and other environmental factors. However, the degree to which ethnicity-associated differences in gut microbial community structure and function are maintained following immigration or in the context of metabolic disease is poorly understood.

Results: We conducted a multi-omic study of 46 lean and obese East Asian (EA) and White (W) participants living in the San Francisco Bay Area. 16S rRNA gene sequencing revealed significant differences between ethnic groups in bacterial richness and community structure. W individuals were enriched for the mucin-degrading *Akkermansia muciniphila*. EA participants had increased levels of multiple *Bacteroidetes* species, fermentative pathways detected by metagenomics, and the short-chain fatty acid end products acetate, propionate, and isobutyrate. Differences in the gut microbiota between the EA and W groups could not be explained by reported dietary intake, were more pronounced for lean individuals, and were associated with current geographical location. Microbiome transplantations into germ-free mice confirmed that the differences in the gut microbiota of the EA and W individuals we analyzed are indeed independent of diet and that they differentially impact host body weight and adiposity in genetically identical mouse recipients.

Conclusions: The reported findings emphasize the utility of studying diverse ethnic groups within a defined geographical location and provide a starting point for dissecting the mechanisms contributing to the complex interactions between the gut microbiome and ethnicity-associated lifestyle, demographic, metabolic, and genetic factors.

Keywords: human gut microbiome, ethnicity, multi-omics, metabolic syndrome, obesity, biogeography

BACKGROUND

Culture-independent surveys have emphasized differences in gut microbial community structure between countries [1–3]; however, the factors that contribute to these differences are poorly understood. Diet is a common hypothesis for geographical variations in the gut microbiota [4,5], based upon extensive data from intervention experiments in humans and mouse models [6–9]. However, diet is just one of the many factors that distinguishes human populations at the global scale, motivating the desire for a more holistic approach. Self-identified race/ethnicity (SIRE) provides a useful alternative, as it integrates the broader national or cultural tradition of a given social group. Multiple studies have reported associations between the gut microbiota and ethnicity in China [10], the Netherlands [11], Singapore [12], and the United States [13,14]. In contrast, a recent study of Asian immigrants suggested that once an individual relocates to a new country, the microbiota rapidly assumes the structure of the country of residence [3]. Thus, the degree to which microbiome signatures of ethnicity persist following immigration and their consequences for host pathophysiology remain an open question.

The links between ethnicity and metabolic disease are well-established. For example, EA subjects are more likely to develop health-related metabolic complications at lower body mass index (BMI) compared to their W counterparts [15,16]. Moreover, Asian Americans have persistent ethnic differences in metabolic phenotypes following immigration [17], including a decoupling of BMI from total body fat percentage [18]. The mechanisms contributing to these

ethnic differences in fat accrual remain unknown. Human genetic polymorphisms may play a role [19,20]; however, putative alleles are often shared between members of different ethnic groups [21]. The gut microbiome might offer a possible explanation for differences in metabolic disease rates across ethnic groups, but there has been a relative scarcity of microbiome studies in this area.

These observations led us to hypothesize that ethnicity-associated differences in host metabolic phenotypes may be determined by corresponding differences in the gut microbiome. First, we sought to better understand the extent to which ethnicity is linked to the human gut microbiome in states of health and disease. We conducted a cross-sectional multi-omic analysis of the gut microbiome using paired 16S rRNA gene sequencing (16S-seq), metagenomics, and metabolomics from the Inflammation, Diabetes, Ethnicity, and Obesity (IDEO) cohort at the University of California, San Francisco. IDEO includes rich metabolic, dietary, and socioeconomic metadata [18], a restricted geographical distribution within the San Francisco Bay Area, and a balanced distribution of EA and W individuals that are both lean and obese (**Table S1**). We report marked differences in gut microbial richness, community structure, and metabolic end products between EA and W individuals in the IDEO cohort. We then used microbiome transplantations to assess the stability of ethnicity-associated differences in the gut microbiota in the context of genetically identical mice fed the same diet. We also explored the functional consequences of these differences on host metabolic phenotypes. Our results emphasize the importance of considering ethnicity in microbiome research and further complicate prior links between metabolic disease and the gut microbiome [22–24], which may be markedly different across diverse ethnic groups.

METHODS

Human subjects

All study participants were part of the IDEO cohort, which has been previously described [18,25]. Briefly, IDEO consists of 25-65 year-old men and women of multiple ethnicities and across a wide BMI range (18.5–52 kg/m^2) living in the San Francisco Bay Area; exclusion factors include smoking, unstable weight within the last 3 months (>3% weight gain or loss), a diagnosed inflammatory or infectious disease, liver failure, renal dysfunction, cancer, and reported alcohol consumption of >20 grams per day. Using IDEO, we recruited both lean and obese W and EA individuals into this study based on World Health Organization cut-offs: W/EA BMI≤24.9 kg/m^2 (lean); W BMI≥30 kg/m^2 (obese); and EA BMI≥27.5 kg/m^2 (obese) [17,26,27].

Each participant consented to take part in the study, which was approved by the University of California San Francisco (UCSF) Institutional Review Board. We utilized demographic, medical, dietary, and lifestyle metadata on each participant that were part of their initial recruitment into IDEO, as previously reported [18,25,28]. Participants with Type 2 Diabetes (T2D) were classified in accordance with American Diabetes Association Standards of Medical Care guidelines [29], defined by having glycated hemoglobin (HbA1c) ≥6.5% or the combination of a prior diagnosis of T2D and the active use of an antidiabetic medication.

Anthropometric and body composition measurements

We leverage host phenotypic and demographic data from IDEO, which was the focus of two previous studies [18,25]. For the convenience of the reader, we have reproduced our methods here. Height and weight were measured using a standard stadiometer and scale, and BMI (kg/m^2)

was calculated from two averaged measurements. Waist and hip circumferences (to the nearest 0.5 cm) were measured using a plastic tape meter at the level of the umbilicus and of the greater trochanters, respectively, and waist-to-hip ratio (WHR) was calculated. Blood pressure was measured with a standard mercury sphygmomanometer on the left arm after at least 10 minute of rest. Mean values were determined from two independent measurements. Blood samples were collected after an overnight fast and analyzed for plasma glucose, insulin, serum total cholesterol, high density lipoprotein (HDL) cholesterol, and triglycerides. Low density lipoprotein (LDL) cholesterol was estimated according to the Friedewald formula [30]. Insulin resistance was estimated by the homeostatic model assessment of insulin resistance (HOMA-IR) index calculated from fasting glucose and insulin values [31]. Two obese subjects on insulin were included in the HOMA-IR analysis (1 EA, 1 W). Body composition of the subjects was estimated by Dual-Energy X-ray Absorptiometry (DEXA) using a Hologic Horizon/A scanner (3-minute whole-body scan, <0.1 G milligray) per manufacturer protocol. A single technologist analyzed all DEXA measurements using Hologic Apex software (13.6.0.4:3) following the International Society for Clinical Densitometry guidelines. Visceral adipose tissue (VAT) was estimated from a 5 cm-wide region across the abdomen just above the iliac crest, coincident with the fourth lumbar vertebrae, to avoid interference from iliac crest bone pixels and matching the region commonly used to analyze VAT mass by CT scan [32–34] .

Dietary assessment

IDEO participants completed two dietary questionnaires, as previously described [18,25], allowing for the assessment of usual total fiber intake and fiber from specific sources, as well as macronutrient, phytochemical, vitamin, and mineral uptake. The first instrument was an

Automated Self-Administered 24-hour Dietary Assessment (ASA24) [35,36], which queries intake over a 24-hour period. The 24-hour recalls and supplement data were manually entered in the ASA24 Dietary Assessment Tool (v. 2016), an electronic data collection and dietary analysis program. ASA24 employs research-based strategies to enhance dietary recall using a respondent-driven approach allowing initial recall to be self-defined. The second instrument was the National Cancer Institute's Diet History Questionnaire III (DHQIII) [37,38]. This questionnaire queries one's usual diet over the past month [38]. Completion of DHQIII added significantly to participant survey fatigue, and completion rates were 42% for 1 recall, 79% for 2 recalls and 100% for 3 or 4 recalls after the first 5 months. Ultimately, our protocol was modified to request the completion of the ASA24 at three separate times, at appointments where there are computers and personnel assistance for online completion, as well as the DHQIII questionnaire.

DNA extraction

Human stool samples were homogenized with bead beating for 5 min (Mini-Beadbeater-96, BioSpec) using beads of mixed size and material (Lysing Matrix E 2mL Tube, MP Biomedicals) in the digestion solution and lysis buffer of a Wizard SV 96 Genomic DNA kit (Promega). The samples were centrifuged for 10 min at 16,000 g and the supernatant was transferred to the binding plate. The DNA was then purified according to the manufacturer's instructions. Mouse fecal pellets were homogenized with bead beating for 5 min (Mini-Beadbeater-96, BioSpec) using the ZR BashingBead lysis matrix containing 0.1 and 0.5 mm beads (ZR-96 BashingBead Lysis Rack, Zymo Research) and the lysis solution provided in the ZymoBIOMICS 96 MagBead DNA Kit (Zymo Research). The samples were centrifuged for 5 min at 3,000 g and the supernatant was transferred to 1 mL deep-well plates. The DNA was then purified using the

ZymoBIOMICS 96 MagBead DNA Kit (Zymo Research) according to the manufacturer's instructions.

16S rRNA gene sequencing and analysis

For human samples, 16S rRNA gene amplification was carried out using GoLay-barcoded 515F/806R primers [39] targeting the V4 region of the 16S rRNA gene according to the methods of the Earth Microbiome Project (earthmicrobiome.org) (**Table S2**). Briefly, 2 µL of DNA was combined with 25 µL of AmpliTaq Gold 360 Master Mix (Fisher Scientific), 5 µL of primers (2 µM each GoLay-barcoded 515/806R), and 18 µL H_2O. Amplification was as follows: 10 min 95°C, 30x (30s 95°C, 30s 50°C, 30s 72°C), and 7 min 72°C. Amplicons were quantified with PicoGreen (Quant-It dsDNA; Life Technologies) and pooled at equimolar concentrations. Aliquots of the pool were then column (MinElute PCR Purification Kit; Qiagen) and gel purified (QIAquick Gel Extraction Kit; Qiagen). Libraries were then quantified (KAPA Library Quantification Kit; Illumina) and sequenced with a 600 cycle MiSeq Reagent Kit (250x150; Illumina) with ~15% PhiX spike-in. For mouse samples, 16S rRNA gene amplification was carried out as per reference protocol and primers [40]. In brief, the V4 region of the 16S rRNA gene was amplified with 515F/806R primers containing common adaptor sequences, and then the Illumina flow cell adaptors and dual indices were added in a secondary amplification step (see **Table S3** for index sequences). Amplicons were pooled and normalized using the SequalPrep Normalization Plate Kit (Invitrogen). Aliquots of the pool were then column (MinElute PCR Purification Kit, Qiagen) and gel purified (QIAquick Gel Extraction Kit, Qiagen). Libraries were then quantified and sequenced with a 600 cycle MiSeq Reagent Kit (250x250; Illumina) with ~15% PhiX spike-in.

Demultiplexed sequencing reads were processed using QIIME2 v2020.2 (qiime2.org) with denoising by DADA2 [41]. Taxonomy was assigned using the DADA2 implementation of the RDP classifier [42] using the DADA2 formatted training sets for SILVA version 128 (benjjneb.github.io/dada2/assign.html). Amplicon sequence variants (ASVs) were filtered such that they were present in more than one sample with at least a total of 10 reads across all samples. Alpha diversity metrics were calculated on subsampled reads using Vegan [43] and Picante [44] R packages. The PhILR Euclidean distance was calculated by first carrying out the phylogenetic isometric log ratio transformation (philr, PhILR [45]) followed by calculating the Euclidean distance (vegdist, Vegan [43]). Principal coordinates analysis was carried out using the pcoa function of APE [46]. ADONIS calculations were carried out (adonis, Vegan) with 999 replications on each distance metric. Centered $\log_2$-ratio (CLR) normalized abundances were calculated using the Make.CLR function in MicrobeR package [47] with count zero multiplicative replacement (zCompositions; [48]). ALDEx2 [49] was used to analyze differential abundances of count data, using features that represented at least 0.05% of total sequencing reads. Corrections for multiple hypothesis testing to false discovery rate (FDR) using the Benjamin-Hochberg method [50] were performed where applicable. Analysis of distance matrices and alpha diversity mirror prior analyses developed in the Turnbaugh lab and were adapted to the current manuscript [9]. Calculations of associations between ASVs and ASA24 questionnaire data were completed by calculating a Spearman rank correlation and then adjusting the *p*-value for a Benjamini-Hochberg FDR using the cor_pmat function in the R package ggcorrplot.

205

206 **Metagenomic sequencing and analysis**

207 Whole-genome shotgun libraries were prepared using the Nextera XT DNA Library Prep Kit
208 (Illumina). Paired ends of all libraries were sequenced on the NovaSeq 6000 platform in a single
209 sequencing run (n=45 subjects; see **Table S2** for relevant metadata and statistics). Illumina reads
210 underwent quality trimming and adaptor removal using fastp [51] and host read removal using
211 BMTagger v1.1.0 (ftp.ncbi.nlm.nih.gov/pub/agarwala/bmtagger/) in the metaWRAP pipeline
212 (github.com/bxlab/metaWRAP). Metagenomic samples were taxonomically profiled using
213 MetaPhlan2 v2.7.7 [52] and functionally profiled using HUMAnN2 v0.11.2 [53], both with
214 default parameters. Principal coordinates analysis on MetaPhlan2 species-level abundances was
215 carried out using Bray Curtis distances and the pcoa function of APE [46]. Tables of gene family
216 abundances from HUMAnN2 were regrouped to KEGG orthologous groups using
217 humann2_regroup_table. Functional pathways relating to short-chain fatty acid production were
218 manually curated from the pathway outputs from HUMANn2 and normalized by the estimated
219 genome equivalents in each microbial community obtained from MicrobeCensus [54].

220

221 **Quantification of bacterial load**

222 Quantitative PCR (qPCR) was performed on DNA extracted from the human stool samples.
223 DNA templates were diluted to 5 ng/µL before qPCR of total 16S rRNA gene copies was carried
224 out in triplicate 10 µL reactions with 200 nM 340F/514R primers using a BioRad CFX384
225 thermocycler with SYBR Select for CFX Master Mix (Life Technologies) according to the
226 manufacturer's instructions and an annealing temperature of 60˚C. Absolute quantifications were
227 determined against a standard curve of purified 8F/1542R amplified *Akkermansia muciniphila*

DNA. Mean values of triplicate reactions were taken for further downstream analyses. Absolute bacterial abundance was derived by adjustments for dilutions during DNA extraction and template normalization dividing by the total fecal mass used for DNA extraction in grams.

Nuclear magnetic resonance (NMR) metabolomics

NMR spectroscopy was performed at 298K on a Bruker Avance III 600MHz spectrometer configured with a 5 mm inverse cryogenic probe (Bruker Biospin, Germany) as previously described [55]. 50 mg of human feces were extracted with 1 mL of phosphate buffer (K_2HPO_4/NaH_2PO_4, 0.1 M, pH 7.4, 50% v/v D_2O) containing 0.005% sodium 3-(trimethylsilyl) [2,2,3,3-2H4] propionate (TSP-d_4) as a chemical shift reference (δ 0.00). Samples were freeze-thawed three times with liquid nitrogen and water bath for thorough extraction, then homogenized (6500 rpm, 1 cycle, 60 s) and centrifuged (11,180 g, 4 °C, 10 min). The supernatants were transferred to a new 2 mL tube. An additional 600 µL of PBS was added to the pellets, followed by the same extraction procedure described above. Combined fecal extracts were centrifuged (11,180 g, 4°C, 10 min), 600 µL of the supernatant was transferred to a 5 mm NMR tube (Norell, Morganton, NC) for NMR spectroscopy analysis. A standard one-dimensional NOESY pulse sequence noesypr1d (recycle delay-90°-t1-90°-tm-90°-acquisition) is used with a 90 pulse length of approximately 10s (-9.6 dbW) and 64 transients are recorded into 32k data points with a spectral width of 9.6 KHz. NMR spectra were processed as previously described [55]. First, spectra quality was improved with Topspin 3.0 (Bruker Biospin, Germany) for phase and baseline correction and chemical shift calibration. AMIX software (version: 3.9.14, Bruker Biospin, Germany) was used for bucketing (bucket width 0.004 ppm), removal of

250 interfering signal, and scaling (total intensity). Relative concentrations of identified metabolites
251 were obtained by normalized peak area.
252
253 **Targeted gas chromatography mass spectrometry (GC-MS) assays**
254 Targeted analysis of short-chain fatty acids (SCFAs) and branched-chain amino acids (BCAAs)
255 was performed with an Agilent 7890A gas chromatograph coupled with an Agilent 5975 mass
256 spectrometer (Agilent Technologies Santa Clara, CA) using a propyl esterification method as
257 previously described [55]. 50 mg of human fecal samples were pre-weighed, mixed with 1 mL of
258 0.005 M NaOH containing 10 μg/mL caproic acid-6,6,6-d3 (internal standard) and 1.0 mm
259 diameter zirconia/silica beads (BioSpec, Bartlesville, OK). The mixture was thoroughly
260 homogenized and centrifuged (13,200 g, 4°C, 20 min). 500 μL of supernatant was transferred to
261 a 20 mL glass scintillation vial. 500 μL of 1-propanol/pyridine (v/v=3/2) solvent was added into
262 the vial, followed by a slow adding of an aliquot of 100 μL of esterification reagent propyl
263 chloroformate. After a brief vortex of the mixture for 1 min, samples were derivatized at 60°C
264 for 1 hour. After derivatization, samples were extracted with hexane in a two-step procedure
265 (300 μL + 200 μL) as described [56]. First, 300 μL of hexane was added to the sample, briefly
266 vortexed and centrifuged (2,000g, 4°C, 5 min), and 300 μL of the upper layer was transferred to
267 a glass autosampler vial. Second, an additional 200 μL of hexane was added to the sample,
268 vortexed, centrifuged, and the 200 μL upper layer was transferred to the glass autosampler vial.
269 A combination of 500 μL of extracts were obtained for GC-MS analysis. A calibration curve of
270 each SCFA and BCAA was generated with series dilution of the standard for absolute
271 quantitation of the biological concentration of SCFAs and BCAAs in human fecal samples.
272

Targeted bile acid quantitation by UPLC-MS/MS

Bile acid quantitation was performed with an ACQUITY ultra performance liquid chromatography (UPLC) system using a Ethylene Bridged Hybrid C8 column (1,7 µm, 100 mm x 2.1 mm) coupled with a Xevo TQ-S mass spectrometer equipped with an electrospray ionization (ESI) source operating in negative mode (All Waters, Milford, MA) as previously described [57]. Selected ion monitoring (SIM) for non-conjugated bile acids and multiple reaction monitoring (MRM) for conjugated bile acids was used. 50 mg of human fecal sample was pre-weighed, mixed with 1 mL of pre-cooled methanol containing 0.5 µM of stable-isotope-labeled bile acids (internal standards) and 1.0 mm diameter zirconia/silica beads (BioSpec, Bartlesville, OK), followed by thorough homogenization and centrifugation. Supernatant was transferred to an autosampler vial for analysis. 100 µL of serum was extracted by adding 200 µL pre-cooled methanol containing 0.5 µM deuterated bile acids as internal standards. Following centrifugation, the supernatant of the extract was transferred to an autosampler vial for quantitation. Calibration curves of individual bile acids were drafted with bile acid standards for quantitation of the biological abundance of bile acids.

Gnotobiotic mouse experiments

All mouse experiments were approved by the UCSF Institutional Animal Care and Use Committee and performed accordingly. Germ-free mice were maintained within the UCSF Gnotobiotic Core Facility and fed *ad libitum* autoclaved standard chow diet (Lab Diet 5021). Germ-free adult male C57BL/6J mice between 6-10 weeks of age were used for all the experiments described in this paper. 10 lean subjects in our IDEO cohort were selected as donors for the microbiota transplantation experiments, including 5 EA and 5 W donors. Donors matched

for phenotypic data to the degree possible were selected (**Table S4**) for gnotobiotic experiments. Stool samples to be used for transplantation were resuspended in 10 volumes (by weight) of brain heart infusion media in an anaerobic Coy chamber. Each diluted sample was vortexed for 1 min and left to settle for 5 min, and a single 200 µL aliquot of the clarified supernatant was administered by oral gavage into each germ-free mouse recipient. In experiments LFPP1 and LFPP2, microbiome transplantations were performed for 2 donors per experiment (1 W, 1 EA) with gnotobiotic mice housed in sterile isolators (CBC flexible, softwall isolator) and maintained on *ad libitum* standard chow also known as low-fat, high-plant-polysaccharide (LFPP) diet. In LFPP1, 6 germ-free mice per colonization group received an aliquot of stool from a donor of either ethnicity and body composition (measured using EchoMRI) were recorded on the day of colonization and at 6 weeks post-transplantation (per group n=6 recipient mice, 1 isolator, 2 cages). In LFPP2, we shortened the colonization time to 3 weeks and used two new donor samples. For the third experiment (HFHS experiment), mice were fed an irradiated high-fat, high-sugar diet (HFHS, TD.88137, Envigo) at weaning for four weeks prior to colonization and housed in pairs in Tecniplast IsoCages. We included the original 4 donor samples and included 6 new donors (per donor n=2 recipient mice, 1 IsoCage). Body weight and body composition were recorded on the day of colonization and at 3 weeks post-transplantation. Mice were maintained on the HFHS diet throughout the experiment. All samples were sequenced in a single pool (**Table S3**).

Glucose tolerance tests

Food was removed from mice 10 hr (LFPP1 experiment) or 4 hr (HFHS experiment) prior to assessment of glucose tolerance. Mice received i.p. injections of D-glucose (2 mg/kg), followed

by repeated collection of blood by tail nick and determination of glucose levels by handheld glucometer (Abbot Diabetes Care) over a 2-hour period.

Geographic analyses

Map tiles and distance data was obtained using GGMap, OpenStreet Maps, and the Imap R packages. GGMap was employed using a Google Cloud API key and the final map tiles were obtained in July 2020 [58]. Spearman ranked correlation coefficients (*rho)* were calculated as embedded in the R-package GGScatter and GGPlot2. 2018 US Census data for EA and W subjects was obtained (B02001 table for race, data.census.gov) for the ZIP codes available in our study and using the Leaflet package. The census data used is included as part of **Table S2** to aid in reproduction. Each census region is plotted as a percentage of W individuals over a denominator of W and EA subjects. The leaflet package utilized ZIP Code Tabulation Areas (ZCTAs) from the 2010 census. We extracted all ZCTAs starting with 9, and the resulting 29 ZIP codes that overlap with IDEO subjects were analyzed (**Table S2)**. Two ZCTAs (95687 and 95401) were primarily W when comparing W and EA subjects. There were two W subjects recruited from these ZTCAs. These ZIP codes are cut off based on the zoom magnification for that figure and as a result ZTCAs for 27 individuals are plotted. Distance to a central point in SF was calculated. The point of reference was latitude=37.7585102, longitude=-122.4539916. For the San Francisco Bay Bridge the point of reference was latitude=37.7983, longitude= -122.3778.

Dietary questionnaire correlation analysis

DHQIII and ASA24 data were analyzed using a Euclidean distance matrix. These transformations were completed using the cluster package [59]. Subsequent analysis was completed using the vegan package [43]. Procrustes transformations were performed using 16S-seq data from human subjects, which was then subjected to a PhILR transformation. The resulting matrix was rotated against the distance matrix for ASA24 or DHQIII questionnaire data using the procrustes command in the vegan R package using 999 permutations. Mantel statistics were calculated utilizing the mantel command of the vegan package.

R packages used in this study

readxl [60], cluster [59], Rtsne [61], vegan [62], ape [63], ggpubr [64], leaflet [65], tigris [66], MicrobeR [47], OpenStreetMap [67], IMap [68], lmerTest [69], PhILR [45], qiime2R [70], ALDEx2 [49], gghighlight [71], Phyloseq [72], Janitor [73], table 1 [74], Picante [44], ggcorrplot [75].

Statistical analyses

Statistical analysis of the human data was performed using the table1 package in R (STATCorp LLC. College Station, TX). Human data were presented as mean ± SD. Unpaired independent Student's *t* tests were used to compare differences between the two groups in the case of continuous data and in the case of categorical data the χ^2 test was utilized. These tests were adjusted for a Benjamini-Hochberg false discovery rate utilizing the command p.adjust in R, which is indicated as an adjusted *p*-value in the tables. In **Tables S8** and **S9** no values met an adjusted *p*-value cutoff of < 0.1. In **Table S1**, *p*-values indicated by numbers were pooled

together for adjustments and those represented by symbols were separately pooled together for adjustment. All microbiome-related analyses were carried out in R version 3.5.3 or 4.0.2. Where indicated, Wilcoxon rank-sum tests were calculated. A Benjamini-Hochberg false discovery rate of 0.1 was used as the cutoff for statistical significance was utilized in tables as indicated and an FDR of 0.2 was utilized for **Figures S5**. Statistical analysis of glucose tolerance tests was carried out using linear mixed effects models with the lmerTest R package and mouse as random effect. Graphical representation was carried out using ggplot2. Boxplots indicate the interquartile range (25th to 75th percentiles), with the center line indicating the median and whiskers representing 1.5x the interquartile range.

RESULTS

Ethnicity was associated with marked differences in the human gut microbiota. Whereas there were no differences between ethnicities in estimated bacterial content per gram of stool (**Fig. S1A**), principal coordinates analysis of PhILR Euclidean distances from 16S-seq data (**Table S2,** n=22 EA, 24 W subjects) revealed a subtle but significant separation between the gut microbiotas of EA and W subjects (p=0.037, R^2=0.037, ADONIS; **Fig. 1A**). Statistical significance was robust to the distance metric used (**Table S5**). Bacterial diversity, evaluated using three distinct metrics from our 16S-seq data, were all significantly higher in W individuals, including Faith's phylogenetic diversity, ASV richness, and Shannon diversity (**Fig. 1B**). The *Firmicutes* and *Bacteroidetes* phyla were enriched in EA subjects, *Verrucomicrobia* were enriched in W subjects, and *Actinobacteria* and *Proteobacteria* were comparable (**Fig. 1C**). By contrast, analysis at the genus and ASV level did not reveal any differentially abundant groups

between ethnicities, suggesting that the phylum-level trends we observed require the integration of more subtle shifts across multiple component members.

Next, we validated these results by metagenomic sequencing (**Table S2,** n=21 EA, 24 W subjects). Consistent with our 16S-seq analysis, we detected a subtle but significant difference in the gut microbiomes between ethnicities based upon metagenomic species abundances (p=0.025, R^2=0.038, ADONIS) and gene families (p=0.024, R^2=0.040, ADONIS). Visualization of species within each phylum revealed marked variation in the magnitude and direction of change between ethnicities in our metagenomic (**Fig. 1D,E**) and 16S-seq data (**Fig. S1B,C**). Notably, W individuals had higher levels of *Akkermansia muciniphila* (**Fig. 1D,E** and **Fig. S1B,C**), which has been implicated in protection from obesity and its associated metabolic diseases [76].

Next, we used NMR-based stool metabolomics to gain insight into the potential functional consequences of ethnicity-associated differences in the human gut microbiome (**Table S2**, n=10 subjects/ethnicity). Metabolite profiles were more strongly associated with ethnicity (p=0.008, R^2=0.128, ADONIS; **Fig. 2A**) than community structure (R^2=0.033-0.048, ADONIS; **Table S5**) or gene abundance (p=0.024, R^2=0.040, ADONIS). Feature annotations revealed elevated levels of the branched chain amino acid (BCAA) valine and the short-chain fatty acids (SCFAs) acetate and propionate in EA subjects (**Fig. 2B** and **Table S6**). In contrast, proline, formate, alanine, xanthine, and hypoxanthine were found at higher levels in W subjects (**Fig. 2B**). To assess the statistical significance and reproducibility of these trends, we used targeted GC-MS and UPLC-MS/MS to quantify a panel of BCAAs, SCFAs, and bile acids (**Table S7**). Confirming our NMR data, EA subjects had significantly higher levels of stool acetate (**Fig. 2C**) and propionate (**Fig. 2D**); however, we did not detect any significant differences in BCAAs or bile acids **(Fig. S2**). Isobutyrate (which was not detected by NMR) was also significantly higher

in EA subjects (**Fig. 2E**). In agreement with these metabolite levels, a targeted re-analysis of our metagenomic data revealed a significant enrichment in two SCFA-related pathways: "pyruvate fermentation to butanoate" (p=0.023, fold-difference=2.216) and "superpathway of *Clostridium acetobutylicum* acidogenic fermentation" (p=0.023, fold-difference=2.182).

Consistent with prior studies [22,23,77], we found that gut bacterial richness in W individuals was significantly associated with both BMI (**Fig. 3A**) and body fat percentage (**Fig. 3B**). Remarkably, these associations were undetectable in EA subjects (**Figs. 3A,B**) even when other metrics of bacterial diversity were used (**Fig. S3**). Re-analysis of our data separating lean and obese individuals revealed that the previously observed differences between ethnic groups were driven by lean individuals. Lean W subjects had significantly higher bacterial diversity (**Fig. 3C**), in addition to greater differences in both gut microbial community structure (p=0.001, R^2=0.096, ADONIS; **Fig. 3D**) and metabolite profiles (p=0.006, R^2=0.293, ADONIS; **Fig. 3E**), than did corresponding EA individuals. By contrast, obese W vs. EA individuals were not different across any of these metrics (**Figs. 3C-E**). Lean EA individuals were significantly enriched for the *Actinobacteria* and *Firmicutes* phyla with a trend towards increased *Bacteroidetes* (**Fig. 3F**). At the genus level, lean EA subjects had higher levels of *Bacteroides*, *Blautia*, and an unclassified *Lachnospiraceae* taxon (**Figs. 3G,H**). In contrast, the *Verrucomicrobia* phylum (which contains *A. muciniphila*) was consistently enriched in both lean and obese W subjects relative to EA individuals **(Fig. 3F)**.

Next, we sought to understand the potential drivers of differences in the gut microbiome between ethnic groups in lean individuals within the IDEO cohort, focusing on birth location, time spent in the USA, dietary intake, and host metabolic phenotypes. Although everyone in the cohort was recruited from the San Francisco Bay Area, birth location varied widely (**Fig. S4**).

There was no significant difference in the proportion of subjects born in the USA between ethnicities (75% W, 54.5% EA; p=0.15, Pearson's χ^2 test). There was also no significant difference in the geographical distance between birth location and San Francisco [W median 2,318 (2.2-6,906) miles; EA median 1,986 (2.2-6,906) miles; p=0.69, Wilcoxon rank-sum test) or the amount of time spent in the San Francisco Bay Area at the time of sampling [W median 270 (8.00-741) months; EA median 282.5 (8.50-777) years; p=0.42, Wilcoxon rank-sum test). While obese subjects were markedly distinct from lean individuals of both ethnicities with regard to measured metabolic and laboratory parameters (**Table S1**), there were no statistically significant differences between ethnic groups after separating lean and obese individuals (**Table S1**).

Surprisingly, we did not detect any significant differences in either short- (**Table S8**) or long-term (**Table S9**) dietary intake between ethnicities. Consistent with this, Procrustes analysis did not reveal any significant associations between dietary intake and gut microbial community structure: procrustes p=0.452 (DHQIII) and p=0.445 (ASA24) relative to PhILR transformed 16S-seq ASV data. The Spearman Mantel statistic was also non-significant [r=0.09511, p=0.094 (DHQIII) and r=0.02953, p=0.313 (ASA24)], relative to PhILR transformed 16S-seq ASV data. Despite the lack of a strong overall shift in the gut microbiota, we were able to identify 11 ASVs associated with dietary intake in lean W individuals (**Fig. S5**). In contrast, there were no significant ASV-level associations in lean EA subjects.

Given the marked variation in the gut microbiome at the continental scale [1–3], we hypothesized that the observed differences in lean EA and W individuals may be influenced by a participant's current address at the time of sampling. Consistent with this hypothesis, we found clear trends in ethnic group composition across ZIP codes in the IDEO cohort (**Figs. 4A,B**) that

were mirrored by the 2018 US census data (Pearson r=0.52, p=0.026 for neighborhoods with greater than 50% white subjects; **Fig. 4D**). Obese individuals from both ethnicities and lean W subjects tended to live closer to the center of San Francisco relative to lean EA subjects (**Fig. 4C**). Distance between current ZIP code and the center of San Francisco was associated with both gut microbial diversity (**Fig. 4E**) and community structure (**Fig. 4F**). These analyses were robust to the central point used, as shown using the Bay Bridge as the central reference point (**Fig. S6**).

Taken together, our results support the hypothesis that there are stable ethnicity-associated signatures within the gut microbiota of lean EA vs. W individuals that are independent of diet. To experimentally test this hypothesis, we transplanted the gut microbiota of a representative lean W and lean EA individual into germ-free C57BL/6J mice (**Fig. 5A** and **Table S4**). Despite maintaining the genetically identical recipient mice on the same autoclaved low-fat, high plant-polysaccharide (LFPP) diet, we detected significant differences in gut microbial community structure (**Fig. 5B**), bacterial richness (**Fig. 5C**), and taxonomic abundance (**Figs. 5D-E**) between the two ethnicity-specific recipient groups, reflecting the differences we saw when initially analyzing the stool samples of the human participants themselves. A replication experiment using an independent pair of donors revealed similar trends, though they did not reach statistical significance (**Fig. S7**). To assess the reproducibility of these findings across multiple donors and in the context of a distinctive dietary pressure, we next fed 20 germ-free mice a high-fat, high-sugar (HFHS) diet for 4 weeks prior to colonization with microbiota from a W vs. EA donor, and then maintained the mice on this diet following colonization (per group n=10 mice, 5 donors; per donor n=2 mice, 1 cage; **Fig. 5F**). Remarkably, this experiment replicated our original findings on the LFPP diet, including altered gut microbial community

structure (**Fig. 5G**), increased richness in mice receiving W donor microbiota (**Fig. 5H**), and higher levels of *Bacteroides* in mice receiving EA donor gut microbiota (**Figs. 5I-J**).

Moreover, mice transplanted with gut microbiomes of EA and W individuals displayed significant differences in body composition. Mice that received W donor microbiota and were fed the LFPP diet gained more body weight (**Fig. 6A**) and increased their adiposity (**Fig. 6B**), in conjunction with a reduction in lean mass (**Fig. 6C**), relative to mice that received the EA donor microbiota. These overall trends were mirrored in the human microbiota recipient mice that were fed the HFHS diet **(Figs. 6E-G)**, though they did not reach statistical significance due to marked variations between donors independent of ethnicity (**Fig. S8**). There were no significant differences in glucose tolerance between mice receiving stool transplants from donors of different ethnicity in either experiment (**Figs. 6D**,**H**).

DISCUSSION

Our findings suggest that despite the potential for immigration to erase some of the geographical structure in the gut microbiome [3], there remain stable long-lasting microbial signatures of ethnicity among W and EA residents of the San Francisco Bay Area. The mechanisms responsible remain to be elucidated. In lean individuals within the IDEO cohort, these differences appear to be independent of immigration status, host phenotype, or dietary intake. Our experiments in inbred germ-free mice support the stability of ethnicity-associated differences in the gut microbiota on both the LFPP and HFHS diets, while also demonstrating that variations in host genetics are not necessary to maintain these signatures, at least over short timescales. Our data also supports a potential role for geographic location of residence in

reinforcing differences in the gut microbiota between ethnic groups. The specific reasons why current location matters remains unclear. It may be reflective of subtle differences in dietary intake (*e.g.*, ethnic foods, food source, or phytochemical content) that are hard to capture using the validated nutritional surveys [78]. Alternative hypotheses include biogeographical patterns in microbial dispersion [79] or a role for socioeconomic factors, which are correlated with neighborhood [80].

Surprisingly, our findings demonstrate that ethnicity-associated differences in the gut microbiota are stronger in lean individuals. Obese individuals did not exhibit as clear a difference in the gut microbiota between ethic groups, either suggesting that established obesity can overwrite long-lasting microbial signatures or alternatively that there is a shared ethnicity-independent microbiome type that predisposes individuals to obesity. Studies in other disease areas (*e.g.*, inflammatory bowel disease and cancer) with similar multi-ethnic cohorts are essential to test the generalizability of these findings and to generate hypotheses as to their mechanistic underpinnings.

Our results in humans and mouse models support the broad potential for downstream consequences of ethnicity-associated differences in the gut microbiome for metabolic syndrome and potentially other disease areas. However, the causal relationships and how they can be understood in the context of the broader differences in host phenotype between ethnicities require further study. While these data are consistent with our general hypothesis that ethnicity-associated differences in the gut microbiome are a source of differences in host metabolic disease, we were surprised by both the nature of the microbiome shifts and their directionality. Based upon observations in the IDEO [18] and other cohorts [15,16], we anticipated that the gut microbiomes of lean EA individuals would promote obesity or other features of metabolic

524 syndrome. In humans, we did find multiple signals that have been previously linked to obesity
525 and its associated metabolic diseases in EA individuals, including increased Firmicutes [9,81],
526 decreased *A. muciniphila* [76,82], decreased diversity [23], and increased acetate [83,84]. Yet
527 EA subjects also had higher levels of *Bacteroidetes* and *Bacteroides*, which have been linked to
528 improved metabolic health [85]. More importantly, our microbiome transplantations
529 demonstrated that the recipients of the lean EA gut microbiome had less body fat despite
530 consuming the same LFPP and HFHS diets. These seemingly contradictory findings may suggest
531 that the recipient mice lost some of the microbial features of ethnicity relevant to host metabolic
532 disease or alternatively that the microbiome acts in a beneficial manner to counteract other
533 ethnicity-associated factors driving disease.

534 EA subjects also had elevated levels of the short chain fatty acids propionate and
535 isobutyrate. The consequences of elevated intestinal propionate levels are unclear given the
536 seemingly conflicting evidence in the literature that propionate may either exacerbate [86] or
537 protect [87] from aspects of metabolic syndrome. Clinical data suggests that circulating
538 propionate may be more relevant for disease than fecal levels [88], emphasizing the importance
539 of considering both the specific microbial metabolites produced, their intestinal absorption, and
540 their distribution throughout the body. Isobutyrate is even less well-characterized, with prior
541 links to dietary intake [89] but no association with obesity [90].

542 There are multiple limitations of this study. Due to the investment of resources into
543 ensuring a high level of phenotypic information on each cohort member, and due to its restricted
544 geographical catchment area, the IDEO cohort was relatively small at the time of this analysis
545 (n=46 individuals). This study only focused on two of the major ethnicities in the San Francisco
546 Bay Area; as IDEO continues to expand and diversify its membership, we hope to study a

sufficient number of participants from other ethnic groups in the future. Stool samples were collected at a single time point and analyzed in a cross-sectional manner. While we used validated tools from the field of nutrition to monitor dietary intake, we cannot fully exclude subtle dietary differences between ethnicities [91], which would be possible with a controlled feeding study [81]. In our animal studies, we focused on metabolically healthy wild-type germ-free mice. Follow-up studies in the appropriate disease models coupled to controlled experimentation with individual strains or more complex synthetic communities are necessary to elucidate the mechanisms responsible for ethnicity-associated changes in host physiology and their relevance to disease.

CONCLUSIONS

Our results support the utility of considering ethnicity as a covariate in microbiome studies, due to the ability to detect signals that are difficult to capture by more specific metadata such as individual dietary intake values. On the other hand, these findings raise the importance of dissecting the sociological and biological components of ethnicity with the goal of identifying factors that shape the gut microbiota, either alone or in combination. This emerging area of microbiome research is just one component in the broader efforts to explore the boundaries and mechanistic underpinning of ethnicity with respect to multiple ethnic groups. The IDEO cohort provides a valuable research tool to conduct prospective longitudinal and intervention studies examining diabetes including Asian American participants. More broadly, IDEO provides a framework to approach other disease states where self-identified race or ethnicity are thought to contribute to health outcomes related to the microbiome. By understanding the biologic features that drive differences between ethnic groups, we may be able to achieve similar health outcomes

and to support more precise therapies informed by a broader appreciation of both microbial and human diversity.

FIGURE LEGENDS

Figure 1. The gut microbiota is distinct between East Asian and White subjects living in the Bay Area.

(A-C) 16S-seq data for subjects in the IDEO cohort. Each point represents a single individual's gut microbiota (n=22 EA, n=24 W).

(A) Principal coordinate analysis of PhILR Euclidean distances reveals significant separation between ethnic groups (p=0.037, R^2=0.037, ADONIS). Additional distance metrics are shown in **Table S5**.

(B) Microbial diversity metrics are significantly different between EA and W subjects. p-values determined using Wilcoxon rank-sum tests.

(C) Three of the five most abundant bacterial phyla are significantly different between EA and W individuals (p-values determined using Wilcoxon rank-sum test).

(D,E) Metagenomic data (n=21 EA, n=24 W).

(D) Each point represents the average relative abundance for a given species within each ethnic group, connected with a line that is colored by the ethnic group with higher mean abundance of each species: EA (yellow) and W (purple).

(E) Pie charts indicate the proportion of species within each phylum that have greater mean abundance in EA or W subjects.

Figure 2. Metabolomics and targeted mass spectrometry highlight significant differences in bacterial fermentation end-products between ethnicities.

(A) Global profiling of the stool metabolome by proton nuclear magnetic resonance (^{1}H NMR) revealed a significant separation in metabolomic profiles between EA and W individuals (p=0.008, R^2=0.128, ADONIS).

(B) Representative stool metabolites contributing to the separation of stool metabolomic profiles between EA and W individuals (p<0.05, Wilcoxon rank-sum test).

(C-E) Gas chromatography-mass spectrometry analysis of short-chain fatty acids (SCFAs) revealed significantly higher concentrations of acetate **(C)**, propionate **(D)** and isobutyrate **(E)** in the stool samples of EA compared to W individuals. *p*-values determined using Wilcoxon rank-sum tests.

(A-E) n=10 EA and n=10 W individuals.

Figure 3. Ethnicity-associated differences in gut microbial community structure are restricted to lean individuals.

(A,B) Faith's phylogenetic diversity is negatively correlated with (A) BMI and (B) percent body fat in W but not EA individuals (*p*-values and Spearman rank correlation coefficients are shown for each graph).

(C) Microbial diversity metrics were significantly different between lean EA and W individuals, but not for obese subjects of the two ethnicities. *p*-values determined using Wilcoxon rank-sum tests.

(D) Principal coordinate analysis of PhILR Euclidean distances reveals significant separation between the gut microbiotas of EA and W lean individuals (p=0.001, R^2=0.096, ADONIS), with no separation in obese subjects (p=0.7, R^2=0.036, ADONIS).

(E) Global profiling of the stool metabolome by proton nuclear magnetic resonance (^{1}H NMR) stratified by lean and obese individuals reveals a significant difference in the metabolomic profiles of lean EA (n=5) and W (n =5) individuals (p=0.006, R^2=0.293, ADONIS) that is not present in obese individuals (p=0.202, R^2=0.141, ADONIS).

(F) Variation in the abundance of the five most abundant phyla in our 16S-seq data reveal significant differences between lean individuals (*Firmicutes, Actinobacteria*) but not obese individuals between ethnicities. Both lean and obese W individuals had greater *Verrucomicrobia* compared to their EA counterparts.

(G) Volcano plot of ALDEx2 differential abundance testing on genera in stool microbiomes of lean EA versus W individuals, with significantly different (FDR < 0.1) genera highlighted.

(H) Abundances of the three genera found to be significantly different between ethnicity: *Bacteroides*, *Blautia*, and an unknown genus in the *Lachnospiraceae* family.

(A-D, F-H) n=22 EA and n=24 W individuals.

Figure 4. Ethnicity-associated differences in the gut microbiota of lean individuals are linked to geographic location.

(A) Each symbol represents a subject's ZIP code. Symbols are colored by ethnicity with shape representing lean and obese subjects (n=44 subjects).

(B) A subset of ZIP Code Tabulation Areas (ZCTAs) zoomed in to focus on San Francisco are colored by the proportion of each ethnicity (n=27 ZTCAs). The red star indicates a central point (latitude=37.7585102, longitude=-122.4539916) within San Francisco used for distances calculated in (C).

638 **(C)** Distance to the center of San Francisco, which is indicated by a star in (B), for IDEO
639 subjects stratified by ethnicity and BMI (n=9-13 individuals/group, *p*-values indicate Wilcoxon
640 rank-sum test).
641 **(D)** US census data for EA and W residents in ZCTAs from (B) is displayed by ethnic make-up
642 (a total of 489,117 W and 347,200 Asian individuals in these areas).
643 **(E-F)** Linear regressions of metrics assessing microbial diversity **(E)** and principal coordinates
644 developed in PCoA analysis **(F)** against distance of subject's ZIP code to the center of San
645 Francisco. Spearman rank correlation coefficients and *p*-values are shown for each graph.
646
647 **Figure 5: Differences in the human gut microbiota between ethnicities are maintained**
648 **following transplantation to germ-free mice.**
649 **(A,F)** Experimental designs. **(A)** Germ-free mice fed a LFPP diet received an aliquot of stool
650 from a donor of either ethnicity (per donor n=6 recipient mice, 1 isolator, 2 cages). (**F**) 5 lean EA
651 and 5 W donors stool microbial communities were transplanted into 20 germ-free recipient mice
652 fed a HFHS diet (per donor n=2 recipient mice, 1 IsoCage).
653 **(B,G)** Principal coordinate analysis of PhILR Euclidean distances of stool from germ-free
654 recipient mice sampled at (B) six weeks and (G) three weeks post-transplantation. (**B)** p=0.004,
655 R^2=0.630, ADONIS. (**G**) p=0.001, R^2=0.124, ADONIS. Germ-free mice receiving the same
656 donor sample are connected by a dashed line.
657 **(C,H)** Bacterial richness is significantly higher in mice who received stool samples from lean W
658 donors compared to EA donors. *p*-values determined using Wilcoxon rank-sum tests.
659 **(D,I)** Volcano plot of ALDEx2 differential abundance testing on genera in the stool microbiomes
660 between transplant groups. The x-axis represents the fold difference between EA (numerator)

and W (denominator) subjects. The y-axis is proportional to the false discovery rate (FDR). Significantly different genera (FDR < 0.1) are highlighted.

(E,J) Abundance of the *Bacteroides* genus in each experiment with FDR value shown.

Figure 6: Microbiome transplantation of samples from EA and W individuals differentially affects the body composition of genetically identical recipient mice.

See experimental designs and group numbers in **Figs. 5A,F** and donor phenotypic data in **Table S8**.

(A-C, E-G) Percent change in body weight **(A,E)**, fat mass **(B, F)**, and lean mass **(C, G)** relative to baseline are shown. *p*-values determined using Wilcoxon rank-sum tests.

(D,H) Glucose tolerance test results were not significantly different between groups in either experiment. *p*-values determined using linear mixed effects models with mouse as a random effect.

(A-D) n=6 recipient mice per group. **(E-H)** n=10 recipient mice per group.

Figure S1: Similar total colonization level with distinct bacterial relative abundance between East Asian and White subjects.

(A) We did not detect a significant difference in overall gut microbial colonization assessed by qPCR quantification of 16S rRNA gene copies per gram wet weight (n=18 EA, n=22 W, Wilcoxon rank-sum test). Samples with average cycle quantification (Cq) values >30 were excluded from analysis (n=4 EA, n=2 W samples).

(B,C) 16S-seq data (n=22 EA, n=24 W).

683 **(B)** Each point represents the average CLR abundance for a given ASV within each ethnic group,
684 connected with a line that is colored by the ethnic group with higher mean abundance of each
685 ASV: EA (yellow) and W (purple).
686 **(C)** Pie charts indicate the proportion of ASVs from the top panel and within each phylum that
687 have higher mean abundance in EA or W subjects).
688
689 **Figure S2: Stool concentrations of branched-chain amino acids and bile acids are**
690 **comparable between East Asian and White subjects.**
691 We did not detect a significant difference in the concentrations of BCAAs **(A)** or bile acids **(B)**
692 between EA (n=10) and W (n=10) stool samples. Statistical analyses performed using Wilcoxon
693 rank-sum tests.
694
695 **Figure S3. Microbial diversity metrics are negatively correlated with metabolic parameters**
696 **in White but not East Asian individuals**.
697 **(A,B)** Bacterial richness is significantly correlated with (A) BMI and (B) percent body fat in W
698 but not EA individuals.
699 **(C,D)** Shannon diversity is significantly correlated with (C) BMI in both W and EA individuals,
700 and with (D) percent body fat in W but not EA individuals.
701 Spearman rank correlation coefficients and *p*-values are shown for each graph (n=22 EA, n=24
702 W individuals).
703
704 **Figure S4: Birth location of subjects.**

Symbols representing subjects' birth locations are plotted on a world map. The size, shape and color of the symbols represent the number, BMI and ethnicity of subjects at each location.

Figure S5: Identification of ASVs associated with short-term dietary intake.

Spearman's correlation was calculated between all 16S-seq ASVs and ASA24 data for lean W subjects. Colored boxes indicate correlations that met FDR<0.2 and the direction and intensity of the Spearman's correlation are shown with correlation color indicated in the figure legend. No ASVs met this FDR in lean EA subjects.

Abbreviations taken from ASA24: V_LEGUMES, Beans and peas (legumes) computed as vegetables (cup eq.). PF_LEGUMES, Beans and Peas (legumes) computed as protein foods (oz. eq.) Whole grains contain the entire grain kernel, the bran, germ, and endosperm (oz. eq.).

Figure S6: Distance to the Bay Bridge differentiates lean EA and W individuals.

We repeated our analysis in **Fig. 4** using an alternate central point (The San Francisco Bay Bridge, latitude=37.7983, longitude= -122.3778).

(A) Using the current ZIP codes of subjects, lean W subjects lived closer to the Bay Bridge than lean EA subjects and obese subjects of either ethnicity (n=9-13 individuals/group, *p*-values indicate Wilcoxon rank-sum tests).

(B-C) Linear regressions of metrics assessing microbial diversity **(B)** and principal coordinates developed in PCoA analysis **(C)** against distance of subject's ZIP code to the Bay Bridge. Spearman rank correlation coefficients and *p*-values are shown for each graph (n=44 individuals).

Figure S7: Replication experiment assessing gut community structure in mice on the LFPP diet.

(A) Principal coordinate analysis of PhILR Euclidean distances of stool between the two transplant groups (p=0.058, R^2=0.230, ADONIS). Mice from the same donor group are connected by a dashed line.

(B) Bacterial richness in stool communities between the two transplant groups. p-value determined using Wilcoxon rank-sum test.

(C) Volcano plot of ALDEx2 differential abundance testing on genera in the stool communities between transplant groups. The x-axis represents the fold difference between EA (numerator) and W (denominator) subjects. The y-axis is proportional to the false discovery rate (FDR). There was no significant genus based on FDR cutoff of 0.1. *Bacteroides* is labelled on the volcano plot.

(D) CLR abundances of the *Bacteroides* genus. Wilcoxon rank-sum test indicates a significant difference in *Bacteroides* abundance between the two transplant groups.

(A-D) n=6 recipient mice per group, sampled at three weeks post-transplantation.

Figure S8: Donor-specific variations in metabolic phenotypes of gnotobiotic mice transplanted with human microbiota.

Germ-free C57BL/6J mice were housed in pairs in Tecniplast cage isolators and transplanted with microbiota from 5 EA donors [EAD 1-5] and 5 W donors [WD 1-5] (n=20 recipient mice housed in 10 cages; per donor n=2 mice, 1 cage). Percent change in body weight **(A),** fat mass **(B)** and lean mass **(C)** at three weeks after transplantation are shown.

LIST OF ABBREVIATIONS

16S-seq: 16S rRNA gene sequencing

ASA24: Automated Self Administered 24-Hour Dietary Assessment Tool

ASV: Amplicon Sequence Variant

BCAA: branched chain amino acid

BMI: body mass index

DHQIII: Diet History Questionnaire III

EA: East Asian

HFHS: high-fat, high-sugar

LFPP: low-fat, plant-polysaccharide rich

SCFA: short-chain fatty acid

W: White

ZCTA: ZIP Code Tabulation Area

DECLARATIONS

Ethics approval and consent to participate

Human stool samples were collected as part of a multi-ethnic clinical cohort study termed Inflammation, Diabetes, Ethnicity and Obesity (ClinicalTrials.gov identifier NCT03022682), consisting of 25- to 65-year-old men and women residing in Northern California and recruited

774 from medical and surgical clinics at UCSF and the Zuckerberg San Francisco General Hospital,
775 or through local public advertisements. The host phenotypic data from this cohort have been
776 described in detail [18,25]. Informed consent was provided for all subjects participating in the
777 study, which was approved by the UCSF Institutional Review Board. Protocols for all
778 experiments involving mice were approved by the University of California, San Francisco
779 Institutional Animal Care and Use Committee, and performed accordingly.
780

781 **Consent for publication**

782 Not applicable.

783 **Availability of data and materials**

784 All 16S-seq and metagenomic sequencing data generated in the preparation of this manuscript
785 have been deposited in NCBI's Sequence Read Archive under accession number PRJNA665061.
786 Metabolomics results and metadata are available within this manuscript (**Tables S2, S3, S5,** and
787 **S6**). Code for our manuscript will be uploaded to GitHub (https://github.com/turnbaughlab).
788

789 **Competing interests**

790 P.J.T. is on the scientific advisory board for Kaleido, Pendulum, Seres, and SNIPRbiome; there
791 is no direct overlap between the current study and these consulting duties. All other authors
792 declare that they have no competing interests.

793 **Funding**

794 This work was supported by the National Institutes of Health [R01HL122593, R21CA227232,
795 R01AR074500, R01DK114034 (PJT); 1R01DK11230401, R01DK11230403S1, (SKK)]. PJT is
796 a Chan Zuckerberg Biohub investigator and was a Nadia's Gift Foundation Innovator, supported
797 in part by the Damon Runyon Cancer Research Foundation (DRR-42-16). DLA is supported by
798 the American Diabetes Association (1-18-PMF-003). VU is supported by the National Institutes
799 of Health T32HL007185. ADP is supported in part by the Pennsylvania Department of Health
800 using Tobacco CURE funds, and the USDA National Institute of Food and Federal
801 Appropriations under Project PEN04607 and Accession number 1009993. None of these funding
802 bodies played a role in the design of the study, the collection, analysis, and interpretation of data,
803 or in writing the manuscript.

804 **Authors' contributions**

805 PJT and SKK designed the study. DLA and SKK recruited the IDEO cohort. QYA and DLA
806 performed all gnotobiotic mouse experiments. QYA and EB performed DNA extractions and
807 library preparations for sequencing. QYA and VU conducted all bioinformatic analyses
808 including analysis of microbiome, geographic, and dietary datasets. JEB wrote the bioinformatic
809 pipelines for processing 16S-seq and metagenomic data and assisted with data analysis and
810 interpretation. HLL, GW, and EB helped with the annotation and analysis of subjects' metadata
811 and dietary questionnaires. JC and ADP conducted and analyzed metabolomics data. PJT, QYA,
812 and VU wrote the manuscript and prepared the figures with input from all co-authors.

813 **Acknowledgements**

We thank Jessie Turnbaugh and the other UCSF Gnotobiotics Core Facility staff and members of the Koliwad lab for help with the gnotobiotic mouse experiments. We thank the Penn State Metabolomics Facility. We also thank the CZ Biohub Sequencing Platform for sequencing support, as well as all the subjects who participated in this study.

REFERENCES

1. Yatsunenko T, Rey FE, Manary MJ, Trehan I, Dominguez-Bello MG, Contreras M, et al. Human gut microbiome viewed across age and geography. Nature. Nature Publishing Group; 2012;486:222–7.

2. Hehemann J-H, Correc G, Barbeyron T, Helbert W, Czjzek M, Michel G. Transfer of carbohydrate-active enzymes from marine bacteria to Japanese gut microbiota. Nature. Nature Publishing Group; 2010;464:908–12.

3. Vangay P, Johnson AJ, Ward TL, Al-Ghalith GA, Shields-Cutler RR, Hillmann BM, et al. US Immigration Westernizes the Human Gut Microbiome. Cell. Nature Publishing Group; 2018;175:962–72.e10.

4. De Filippo C, Cavalieri D, Di Paola M, Ramazzotti M, Poullet JB, Massart S, et al. Impact of diet in shaping gut microbiota revealed by a comparative study in children from Europe and rural Africa. Proc Natl Acad Sci U S A. 2010;107:14691–6.

5. Devoto AE, Santini JM, Olm MR, Anantharaman K, Munk P, Tung J, et al. Megaphages

834 infect Prevotella and variants are widespread in gut microbiomes. Nat Microbiol. 2019;4:693–
835 700.

836 6. David LA, Maurice CF, Carmody RN, Gootenberg DB, Button JE, Wolfe BE, et al. Diet
837 rapidly and reproducibly alters the human gut microbiome. Nature. 2014;505:559–63.

838 7. Carmody RN, Gerber GK, Luevano JM Jr, Gatti DM, Somes L, Svenson KL, et al. Diet
839 dominates host genotype in shaping the murine gut microbiota. Cell Host Microbe. 2015;17:72–
840 84.

841 8. Gehrig JL, Venkatesh S, Chang H-W, Hibberd MC, Kung VL, Cheng J, et al. Effects of
842 microbiota-directed foods in gnotobiotic animals and undernourished children. Science .
843 2019;365.

844 9. Bisanz JE, Upadhyay V, Turnbaugh JA, Ly K, Turnbaugh PJ. Meta-Analysis Reveals
845 Reproducible Gut Microbiome Alterations in Response to a High-Fat Diet. Cell Host Microbe.
846 2019;26:265–72.e4.

847 10. Khine WWT, Zhang Y, Goie GJY, Wong MS, Liong M, Lee YY, et al. Gut microbiome of
848 pre-adolescent children of two ethnicities residing in three distant cities. Sci Rep. 2019;9:7831.

849 11. Deschasaux M, Bouter KE, Prodan A, Levin E, Groen AK, Herrema H, et al. Depicting the
850 composition of gut microbiota in a population with varied ethnic origins but shared geography.
851 Nat Med. 2018;24:1526–31.

852 12. Xu J, Lawley B, Wong G, Otal A, Chen L, Ying TJ, et al. Ethnic diversity in infant gut
853 microbiota is apparent before the introduction of complementary diets. Gut Microbes.

854 2020;11:1362–73.

855 13. Brooks AW, Priya S, Blekhman R, Bordenstein SR. Gut microbiota diversity across
856 ethnicities in the United States. PLoS Biol. 2018;16:e2006842.

857 14. Sordillo JE, Zhou Y, McGeachie MJ, Ziniti J, Lange N, Laranjo N, et al. Factors influencing
858 the infant gut microbiome at age 3-6 months: Findings from the ethnically diverse Vitamin D
859 Antenatal Asthma Reduction Trial (VDAART). J Allergy Clin Immunol. Elsevier;
860 2017;139:482–91.e14.

861 15. Zheng W, McLerran DF, Rolland B, Zhang X, Inoue M, Matsuo K, et al. Association
862 between body-mass index and risk of death in more than 1 million Asians. N Engl J Med. Mass
863 Medical Soc; 2011;364:719–29.

864 16. Gu D, He J, Duan X, Reynolds K, Wu X, Chen J, et al. Body weight and mortality among
865 men and women in China. JAMA. jamanetwork.com; 2006;295:776–83.

866 17. Jih J, Mukherjea A, Vittinghoff E, Nguyen TT, Tsoh JY, Fukuoka Y, et al. Using appropriate
867 body mass index cut points for overweight and obesity among Asian Americans. Prev Med .
868 Elsevier; 2014;65:1–6.

869 18. Alba DL, Farooq JA, Lin MYC, Schafer AL, Shepherd J, Koliwad SK. Subcutaneous Fat
870 Fibrosis Links Obesity to Insulin Resistance in Chinese Americans. J Clin Endocrinol Metab.
871 academic.oup.com; 2018;103:3194–204.

872 19. Xiang K, Wang Y, Zheng T, Jia W, Li J, Chen L, et al. Genome-wide search for type 2
873 diabetes/impaired glucose homeostasis susceptibility genes in the Chinese: significant linkage to

874 chromosome 6q21-q23 and chromosome 1q21-q24. Diabetes. Am Diabetes Assoc; 2004;53:228–
875 34.

876 20. Wen J, Rönn T, Olsson A, Yang Z, Lu B, Du Y, et al. Investigation of type 2 diabetes risk
877 alleles support CDKN2A/B, CDKAL1, and TCF7L2 as susceptibility genes in a Han Chinese
878 cohort. PLoS One. journals.plos.org; 2010;5:e9153.

879 21. Gravel S, Henn BM, Gutenkunst RN, Indap AR, Marth GT, Clark AG, et al. Demographic
880 history and rare allele sharing among human populations. Proceedings of the National Academy
881 of Sciences. National Acad Sciences; 2011;108:11983–8.

882 22. Ley RE, Turnbaugh PJ, Klein S, Gordon JI. Human gut microbes associated with obesity.
883 Nature. 2006;444:1022–3.

884 23. Turnbaugh PJ, Hamady M, Yatsunenko T, Cantarel BL, Duncan A, Ley RE, et al. A core gut
885 microbiome in obese and lean twins. Nature. 2009;457:480–4.

886 24. Wu H, Tremaroli V, Schmidt C, Lundqvist A, Olsson LM, Krämer M, et al. The Gut
887 Microbiota in Prediabetes and Diabetes: A Population-Based Cross-Sectional Study. Cell Metab.
888 2020;32:379–90.

889 25. Oguri Y, Shinoda K, Kim H, Alba DL, Bolus WR, Wang Q, et al. CD81 Controls Beige Fat
890 Progenitor Cell Growth and Energy Balance via FAK Signaling. Cell. 2020;182:563–77.e20.

891 26. Hsu WC, Araneta MRG, Kanaya AM, Chiang JL, Fujimoto W. BMI cut points to identify at-
892 risk Asian Americans for type 2 diabetes screening. Diabetes Care. Am Diabetes Assoc;
893 2015;38:150–8.

894 27. WHO Expert Consultation. Appropriate body-mass index for Asian populations and its
895 implications for policy and intervention strategies. Lancet. 2004;363:157–63.

896 28. McClung HL, Ptomey LT, Shook RP, Aggarwal A, Gorczyca AM, Sazonov ES, et al.
897 Dietary Intake and Physical Activity Assessment: Current Tools, Techniques, and Technologies
898 for Use in Adult Populations. Am J Prev Med. Elsevier; 2018;55:e93–104.

899 29. American Diabetes Association. 2. Classification and Diagnosis of Diabetes: Standards of
900 Medical Care in Diabetes—2019. Diabetes Care. American Diabetes Association; 2019;42:S13–
901 28.

902 30. Friedewald WT, Levy RI, Fredrickson DS. Estimation of the concentration of low-density
903 lipoprotein cholesterol in plasma, without use of the preparative ultracentrifuge. Clin Chem.
904 academic.oup.com; 1972;18:499–502.

905 31. Matthews DR, Hosker JP, Rudenski AS, Naylor BA, Treacher DF, Turner RC. Homeostasis
906 model assessment: insulin resistance and beta-cell function from fasting plasma glucose and
907 insulin concentrations in man. Diabetologia. Springer; 1985;28:412–9.

908 32. Kaul S, Rothney MP, Peters DM, Wacker WK, Davis CE, Shapiro MD, et al. Dual-Energy
909 X-Ray Absorptiometry for Quantification of Visceral Fat . Obesity. 2012. p. 1313–8.

910 33. Bredella MA, Gill CM, Keating LK, Torriani M, Anderson EJ, Punyanitya M, et al.
911 Assessment of abdominal fat compartments using DXA in premenopausal women from anorexia
912 nervosa to morbid obesity. Obesity . 2013;21:2458–64.

913 34. Neeland IJ, Grundy SM, Li X, Adams-Huet B, Vega GL. Comparison of visceral fat mass

914 measurement by dual-X-ray absorptiometry and magnetic resonance imaging in a multiethnic
915 cohort: the Dallas Heart Study. Nutr Diabetes. nature.com; 2016;6:e221.

916 35. Timon CM, van den Barg R, Blain RJ, Kehoe L, Evans K, Walton J, et al. A review of the
917 design and validation of web- and computer-based 24-h dietary recall tools . Nutrition Research
918 Reviews. 2016. p. 268–80.

919 36. Park Y, Dodd KW, Kipnis V, Thompson FE, Potischman N, Schoeller DA, et al. Comparison
920 of self-reported dietary intakes from the Automated Self-Administered 24-h recall, 4-d food
921 records, and food-frequency questionnaires against recovery biomarkers . The American Journal
922 of Clinical Nutrition. 2018. p. 80–93.

923 37. Millen AE, Midthune D, Thompson FE, Kipnis V, Subar AF. The National Cancer Institute
924 diet history questionnaire: validation of pyramid food servings. Am J Epidemiol. 2006;163:279–
925 88.

926 38. Diet History Questionnaire III (DHQ III). Available from: https://epi.grants.cancer.gov/dhq3/

927 39. Caporaso JG, Lauber CL, Walters WA, Berg-Lyons D, Huntley J, Fierer N, et al. Ultra-high-
928 throughput microbial community analysis on the Illumina HiSeq and MiSeq platforms. ISME J.
929 2012;6:1621–4.

930 40. Gohl DM, Vangay P, Garbe J, MacLean A, Hauge A, Becker A, et al. Systematic
931 improvement of amplicon marker gene methods for increased accuracy in microbiome studies.
932 Nat Biotechnol. 2016;34:942–9.

933 41. Callahan BJ, McMurdie PJ, Rosen MJ, Han AW, Johnson AJA, Holmes SP. DADA2: High-

934 resolution sample inference from Illumina amplicon data. Nat Methods. 2016;13:581–3.

935 42. Wang Q, Garrity GM, Tiedje JM, Cole JR. Naive Bayesian classifier for rapid assignment of
936 rRNA sequences into the new bacterial taxonomy. Appl Environ Microbiol. 2007;73:5261–7.

937 43. Dixon P. VEGAN, a package of R functions for community ecology. J Veg Sci.
938 2003;14:927–30.

939 44. Kembel SW, Cowan PD, Helmus MR, Cornwell WK, Morlon H, Ackerly DD, et al. Picante:
940 R tools for integrating phylogenies and ecology. Bioinformatics. 2010;26:1463–4.

941 45. Silverman JD, Washburne AD, Mukherjee S, David LA. A phylogenetic transform enhances
942 analysis of compositional microbiota data. Elife . elifesciences.org; 2017;6.

943 46. Paradis E, Claude J, Strimmer K. APE: analyses of phylogenetics and evolution in R
944 language. Bioinformatics. 2004;20:289–90.

945 47. Bisanz J. MicrobeR v 0.3.2: Handy functions for microbiome analysis in R. GitHub . 2017.

946 48. Martín-Fernández J-A, Hron K, Templ M, Filzmoser P, Palarea-Albaladejo J. Bayesian-
947 multiplicative treatment of count zeros in compositional data sets. Stat Modelling. SAGE
948 Publications India; 2015;15:134–58.

949 49. Fernandes AD, Macklaim JM, Linn TG, Reid G, Gloor GB. ANOVA-like differential gene
950 expression analysis of single-organism and meta-RNA-seq. PLoS One. 2013;8:e67019.

951 50. Benjamini Y, Hochberg Y. Controlling the false discovery rate: a practical and powerful
952 approach to multiple testing. J R Stat Soc Series B Stat Methodol. Royal Statistical Society,
953 Wiley; 1995;57:289–300.

954 51. Chen S, Zhou Y, Chen Y, Gu J. fastp: an ultra-fast all-in-one FASTQ preprocessor.
955 Bioinformatics. 2018;34:i884–90.

956 52. Segata N, Waldron L, Ballarini A, Narasimhan V, Jousson O, Huttenhower C. Metagenomic
957 microbial community profiling using unique clade-specific marker genes. Nat Methods.
958 2012;9:811–4.

959 53. Franzosa EA, McIver LJ, Rahnavard G, Thompson LR, Schirmer M, Weingart G, et al.
960 Species-level functional profiling of metagenomes and metatranscriptomes. Nat Methods.
961 2018;15:962–8.

962 54. Nayfach S, Pollard KS. Average genome size estimation improves comparative
963 metagenomics and sheds light on the functional ecology of the human microbiome. Genome
964 Biol. 2015;16:51.

965 55. Cai J, Zhang J, Tian Y, Zhang L, Hatzakis E, Krausz KW, et al. Orthogonal comparison of
966 GC-MS and 1H NMR spectroscopy for short chain fatty acid quantitation. Anal Chem.
967 2017;89:7900–6.

968 56. Zheng X, Qiu Y, Zhong W, Baxter S, Su M, Li Q, et al. A targeted metabolomic protocol for
969 short-chain fatty acids and branched-chain amino acids. Metabolomics. 2013;9:818–27.

970 57. Sarafian MH, Lewis MR, Pechlivanis A, Ralphs S, McPhail MJW, Patel VC, et al. Bile acid
971 profiling and quantification in biofluids using ultra-performance liquid chromatography tandem
972 mass spectrometry. Anal Chem. 2015;87:9662–70.

973 58. Kahle D, Wickham H. ggmap: Spatial Visualization with ggplot2. R J. researchgate.net;

974 2013;5:144–61.

975 59. Maechler M, Rousseeuw P, Struyf A, Hubert M, Hornik K, Others. Cluster: cluster analysis
976 basics and extensions. R package version. 2012;1:56.

977 60. Wickham H, Bryan J. readxl: Read Excel Files. R package version 1.0. 0. URL https://CRAN
978 R-project org/package= readxl. 2017.

979 61. Krijthe JH. Rtsne: T-distributed stochastic neighbor embedding using Barnes-Hut
980 implementation. R package version 0 13, URL https://github com/jkrijthe/Rtsne. 2015.

981 62. Oksanen J, Blanchet FG, Kindt R, Legendre P, Minchin PR, O'hara RB, et al. Community
982 ecology package. R package version. sortie-nd.org; 2013;2–0.

983 63. Paradis E, Schliep K. ape 5.0: an environment for modern phylogenetics and evolutionary
984 analyses in R. Bioinformatics . academic.oup.com; 2019.

985 64. Kassambara A. ggpubr:"ggplot2" based publication ready plots. R package version 0 1.
986 2018;7.

987 65. Cheng J, Karambelkar B, Xie Y. Leaflet: Create interactive web maps with the
988 javascript'leaflet'library. R package version. 2018;2.

989 66. Walker K. Tigris: Load census TIGER/Line Shapefiles. R package version 0.7. 2018.

990 67. Fellows I, Stotz JP. OpenStreetMap: Access to open street map raster images. R Package
991 Version, 0.3. 3. 2016.

992 68. Wallace JR. Imap: Interactive mapping. R package version 1.32. R Found Stat Comput;

2012.

69. Kuznetsova A, Brockhoff PB, Christensen RHB, Others. lmerTest package: tests in linear mixed effects models. J Stat Softw. core.ac.uk; 2017;82:1–26.

70. Bisanz JE. qiime2R: Importing QIIME2 artifacts and associated data into R sessions. Version 0 99. 2018;13.

71. Yutani H. gghighlight: Highlight Lines and Points in “ggplot2.” Manual available online at http://CRAN R-project org/package= gghighlight. 2018.

72. McMurdie PJ, Holmes S. phyloseq: an R package for reproducible interactive analysis and graphics of microbiome census data. PLoS One. journals.plos.org; 2013;8:e61217.

73. Firke S. Janitor: Simple tools for examining and cleaning dirty data. R package version. 2018;1.

74. Rich B. table1: Tables of Descriptive Statistics in HTML. R package version 12 . 2020.

75. Kassambara A, Kassambara MA. Package “ggcorrplot.” R package version 0 1 . mran.microsoft.com; 2019;3.

76. Plovier H, Everard A, Druart C, Depommier C, Van Hul M, Geurts L, et al. A purified membrane protein from Akkermansia muciniphila or the pasteurized bacterium improves metabolism in obese and diabetic mice. Nat Med. 2017;23:107–13.

77. Jumpertz R, Le DS, Turnbaugh PJ, Trinidad C, Bogardus C, Gordon JI, et al. Energy-balance studies reveal associations between gut microbes, caloric load, and nutrient absorption in humans. Am J Clin Nutr. 2011;94:58–65.

1013 78. Garduño-Diaz SD, Husain W, Ashkanani F, Khokhar S. Meeting challenges related to the
1014 dietary assessment of ethnic minority populations. J Hum Nutr Diet. Wiley Online Library;
1015 2014;27:358–66.

1016 79. Martiny JBH, Bohannan BJM, Brown JH, Colwell RK, Fuhrman JA, Green JL, et al.
1017 Microbial biogeography: putting microorganisms on the map. Nat Rev Microbiol. nature.com;
1018 2006;4:102–12.

1019 80. Kakar V, Voelz J, Wu J, Franco J. The Visible Host: Does race guide Airbnb rental rates in
1020 San Francisco? J Hous Econ. Elsevier; 2018;40:25–40.

1021 81. Basolo A, Hohenadel M, Ang QY, Piaggi P, Heinitz S, Walter M, et al. Effects of
1022 underfeeding and oral vancomycin on gut microbiome and nutrient absorption in humans. Nat
1023 Med. 2020;26:589–98.

1024 82. Depommier C, Everard A, Druart C, Plovier H, Van Hul M, Vieira-Silva S, et al.
1025 Supplementation with Akkermansia muciniphila in overweight and obese human volunteers: a
1026 proof-of-concept exploratory study. Nat Med. 2019;25:1096–103.

1027 83. Perry RJ, Peng L, Barry NA, Cline GW, Zhang D, Cardone RL, et al. Acetate mediates a
1028 microbiome–brain–β-cell axis to promote metabolic syndrome. Nature. Nature Publishing
1029 Group; 2016;534:213–7.

1030 84. Turnbaugh PJ, Ley RE, Mahowald MA, Magrini V, Mardis ER, Gordon JI. An obesity-
1031 associated gut microbiome with increased capacity for energy harvest. Nature. 2006;444:1027–
1032 31.

1033 85. Johnson EL, Heaver SL, Walters WA, Ley RE. Microbiome and metabolic disease: revisiting
1034 the bacterial phylum Bacteroidetes. J Mol Med . Springer; 2017;95:1–8.

1035 86. Tirosh A, Calay ES, Tuncman G, Claiborn KC, Inouye KE, Eguchi K, et al. The short-chain
1036 fatty acid propionate increases glucagon and FABP4 production, impairing insulin action in mice
1037 and humans. Sci Transl Med . stm.sciencemag.org; 2019;11.

1038 87. Lu Y, Fan C, Li P, Lu Y, Chang X, Qi K. Short Chain Fatty Acids Prevent High-fat-diet-
1039 induced Obesity in Mice by Regulating G Protein-coupled Receptors and Gut Microbiota. Sci
1040 Rep. nature.com; 2016;6:37589.

1041 88. Müller M, Hernández MAG, Goossens GH, Reijnders D, Holst JJ, Jocken JWE, et al.
1042 Circulating but not faecal short-chain fatty acids are related to insulin sensitivity, lipolysis and
1043 GLP-1 concentrations in humans. Sci Rep. nature.com; 2019;9:12515.

1044 89. Berding K, Donovan SM. Diet Can Impact Microbiota Composition in Children With Autism
1045 Spectrum Disorder. Front Neurosci. frontiersin.org; 2018;12:515.

1046 90. Kim KN, Yao Y, Ju SY. Short Chain Fatty Acids and Fecal Microbiota Abundance in
1047 Humans with Obesity: A Systematic Review and Meta-Analysis. Nutrients . mdpi.com; 2019;11.

1048 91. Johnson AJ, Vangay P, Al-Ghalith GA, Hillmann BM, Ward TL, Shields-Cutler RR, et al.
1049 Daily Sampling Reveals Personalized Diet-Microbiome Associations in Humans. Cell Host
1050 Microbe. 2019;25:789–802.e5.

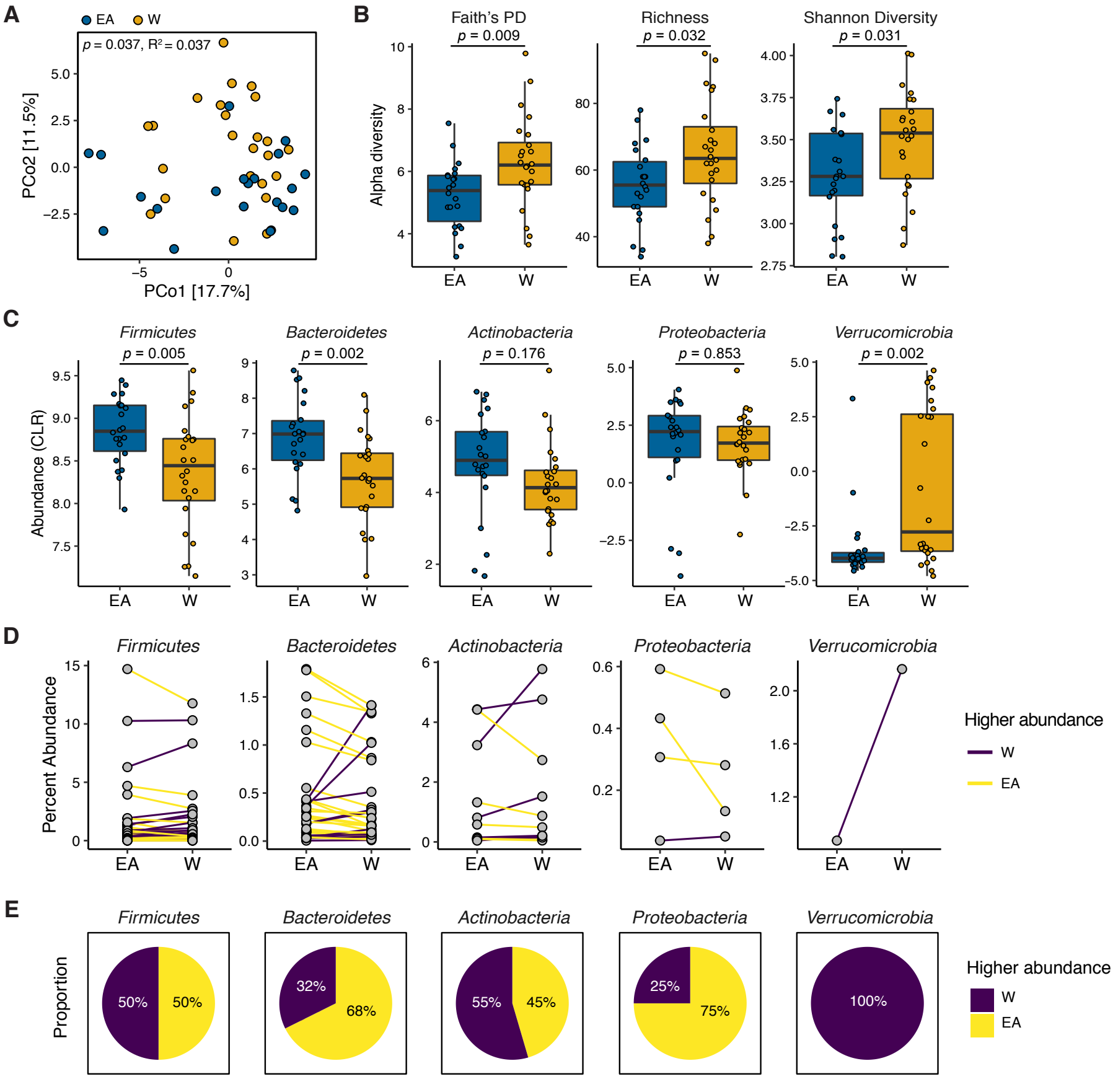
A
EA
W
p = 0.037, R² = 0.037
PCo2 [11.5%]
PCo1 [17.7%]
B
Faith's PD
p = 0.009
Richness
p = 0.032
Shannon Diversity
p = 0.031
Alpha diversity
C
Firmicutes
p = 0.005
Bacteroidetes
p = 0.002
Actinobacteria
p = 0.176
Proteobacteria
p = 0.853
Verrucomicrobia
p = 0.002
Abundance (CLR)
D
Percent Abundance
Higher abundance
W
EA
E
Proportion
50%
50%
32%
68%
55%
45%
25%
75%
100%
Higher abundance
W
EA

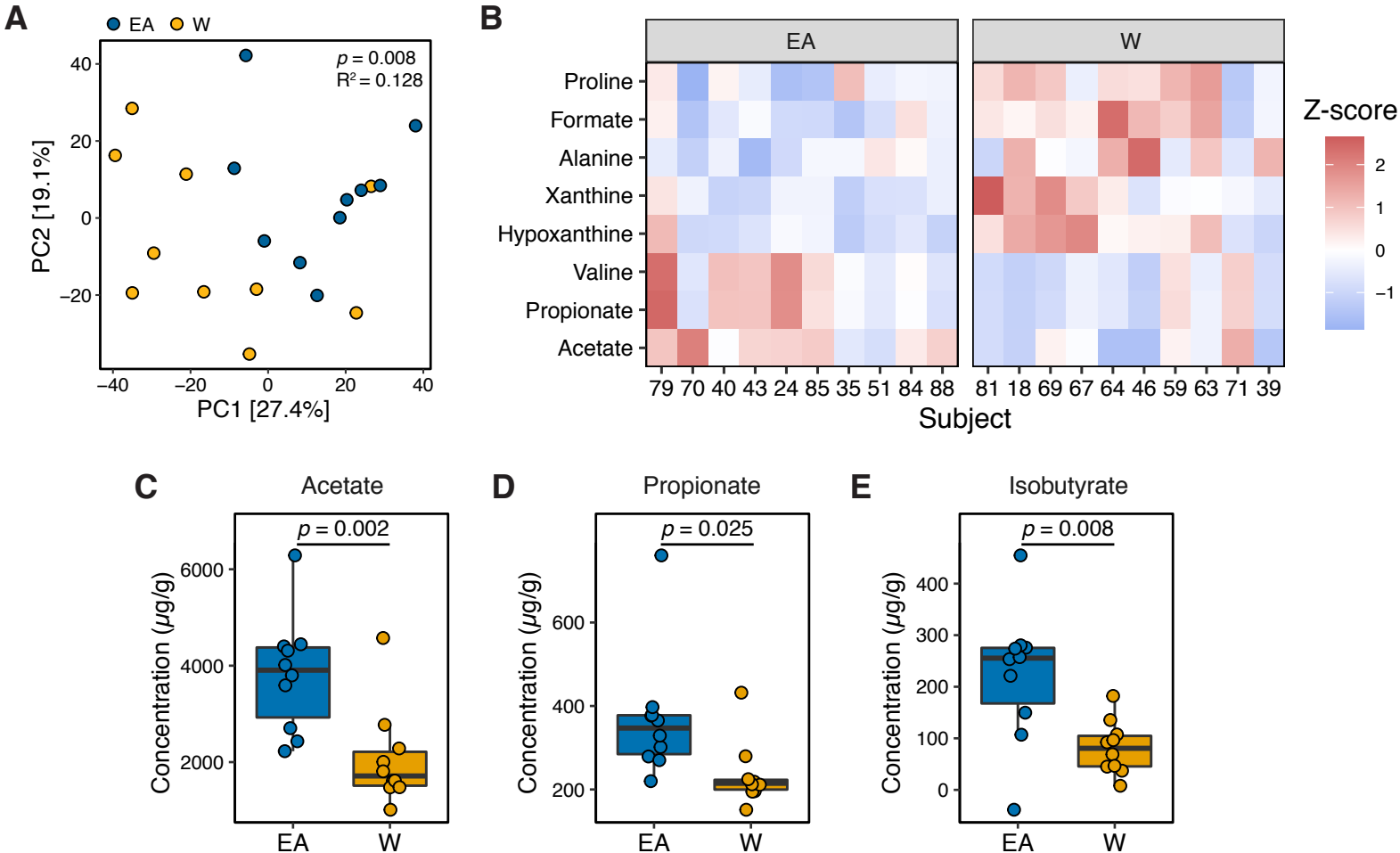
A
EA
W
p = 0.008
R² = 0.128
PC2 [19.1%]
PC1 [27.4%]
B
EA
W
Proline
Formate
Alanine
Xanthine
Hypoxanthine
Valine
Propionate
Acetate
79 70 40 43 24 85 35 51 84 88
81 18 69 67 64 46 59 63 71 39
Subject
Z-score
C
Acetate
p = 0.002
Concentration (μg/g)
D
Propionate
p = 0.025
Concentration (μg/g)
E
Isobutyrate
p = 0.008
Concentration (μg/g)

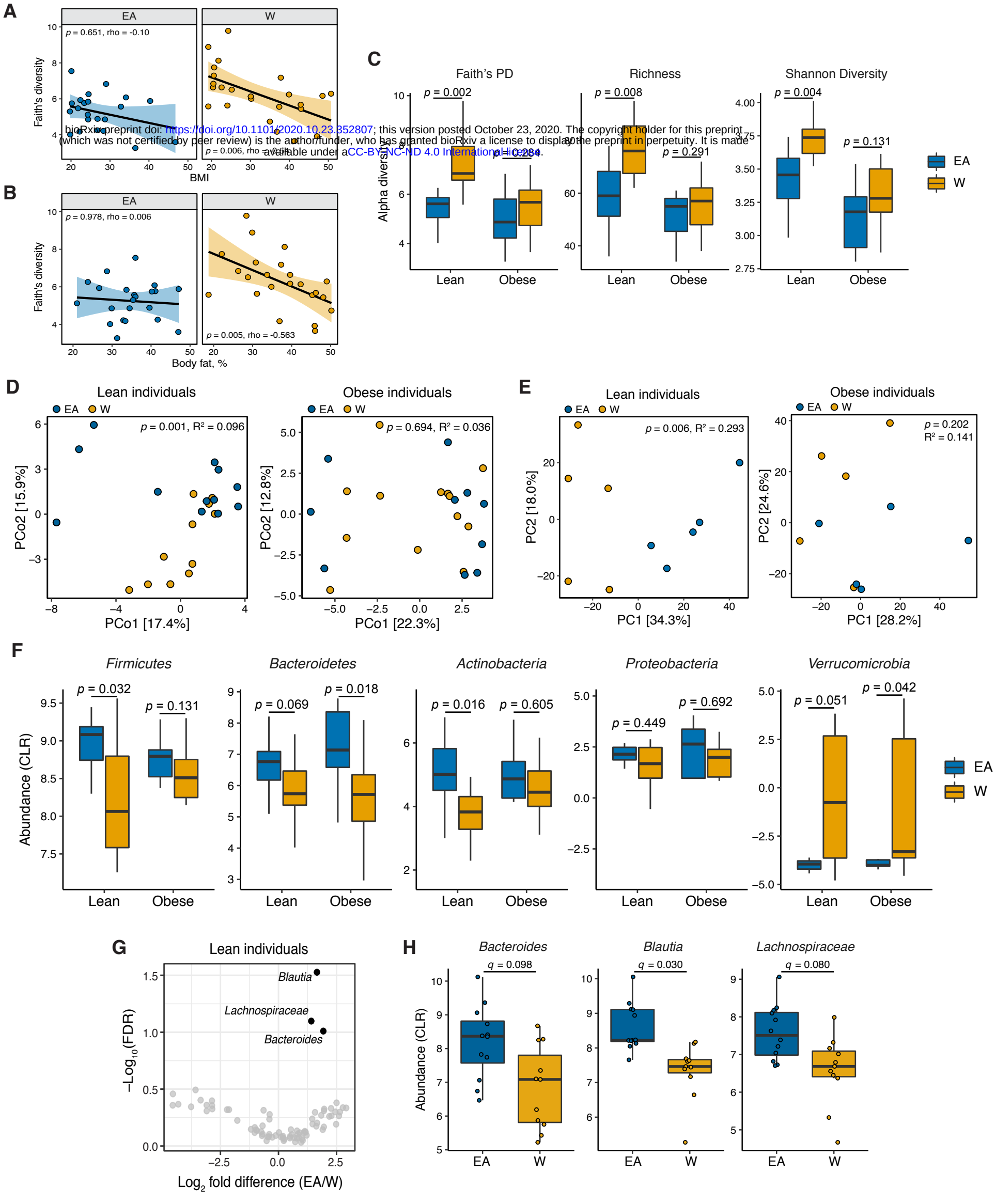

A

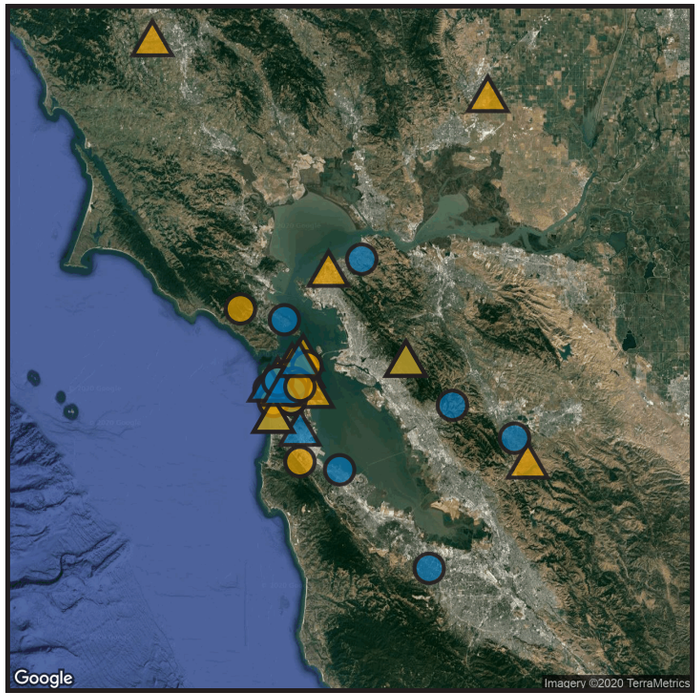
EA
W
Lean
Obese
Google
Imagery ©2020 TerraMetrics

B

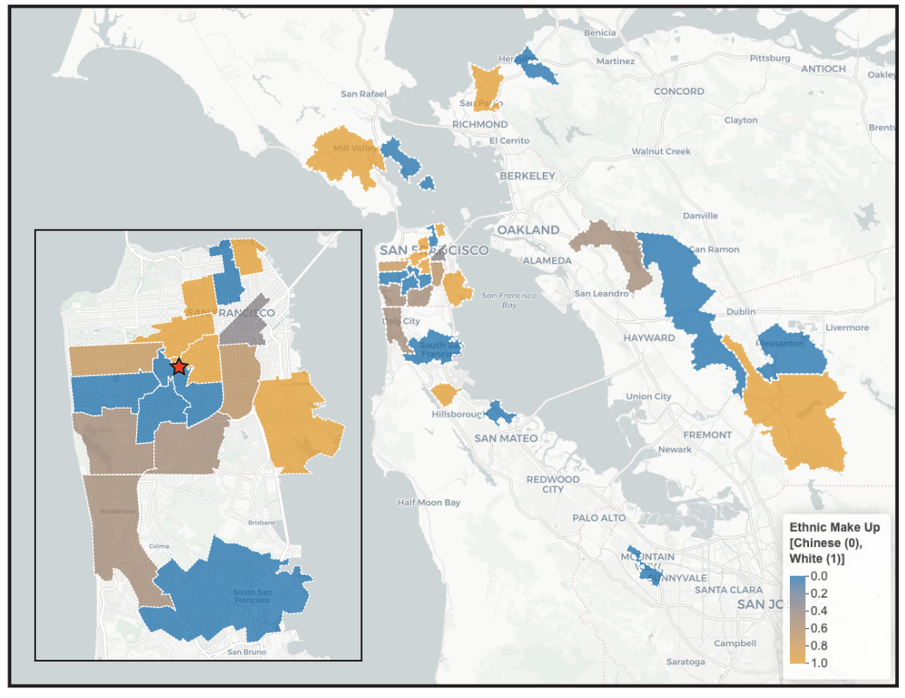
Ethnic Make Up [Chinese (0), White (1)]
0.0
0.2
0.4
0.6
0.8
1.0

C

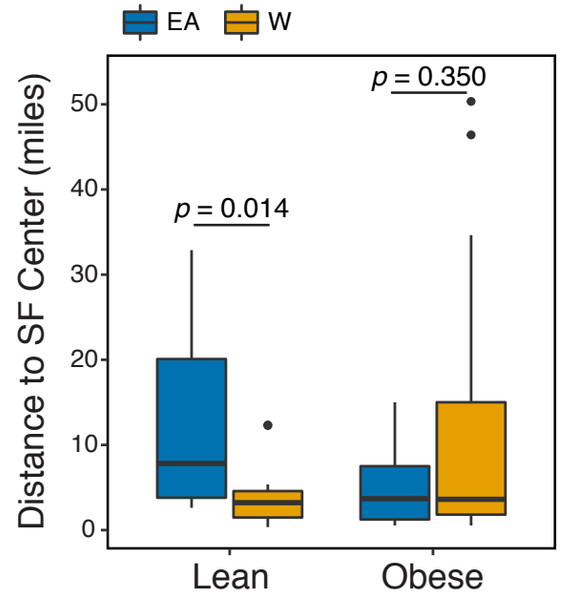
EA
W
Distance to SF Center (miles)
p = 0.014
p = 0.350
Lean
Obese

D

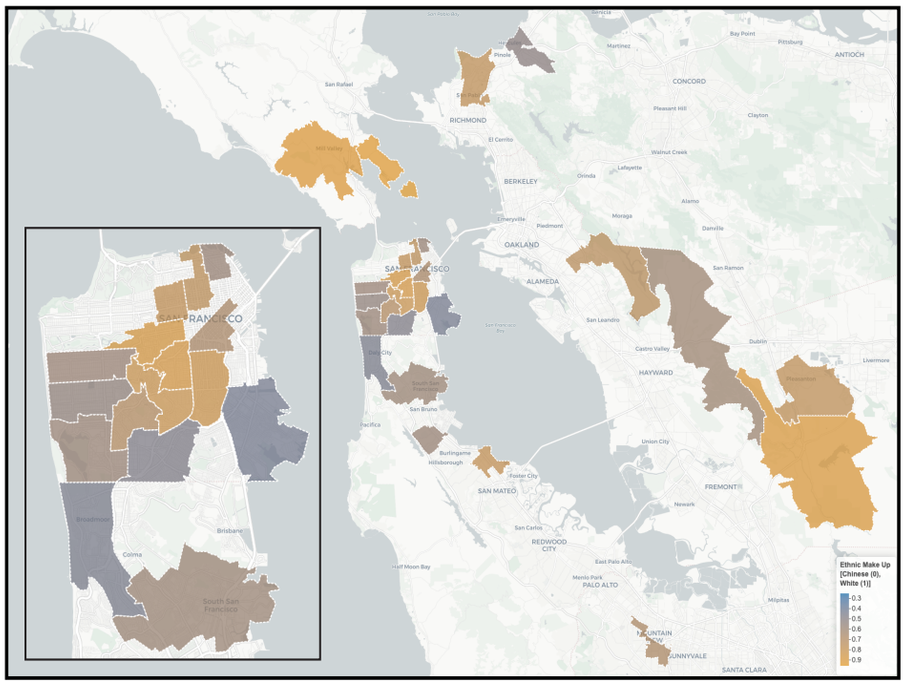
Ethnic Make Up [Chinese (0), White (1)]

E

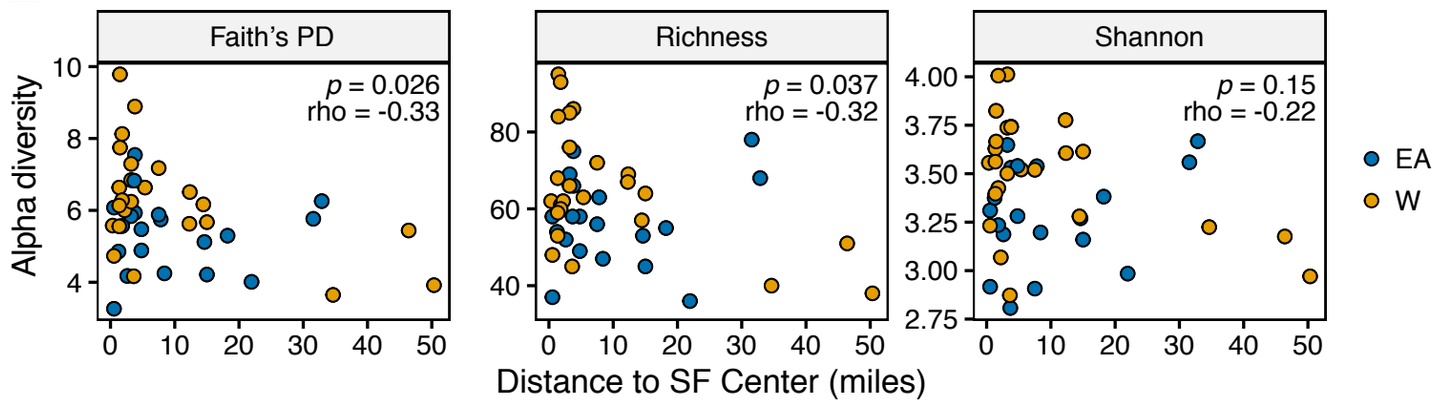
Faith's PD
p = 0.026
rho = -0.33
Richness
p = 0.037
rho = -0.32
Shannon
p = 0.15
rho = -0.22
Alpha diversity
Distance to SF Center (miles)
EA
W

F

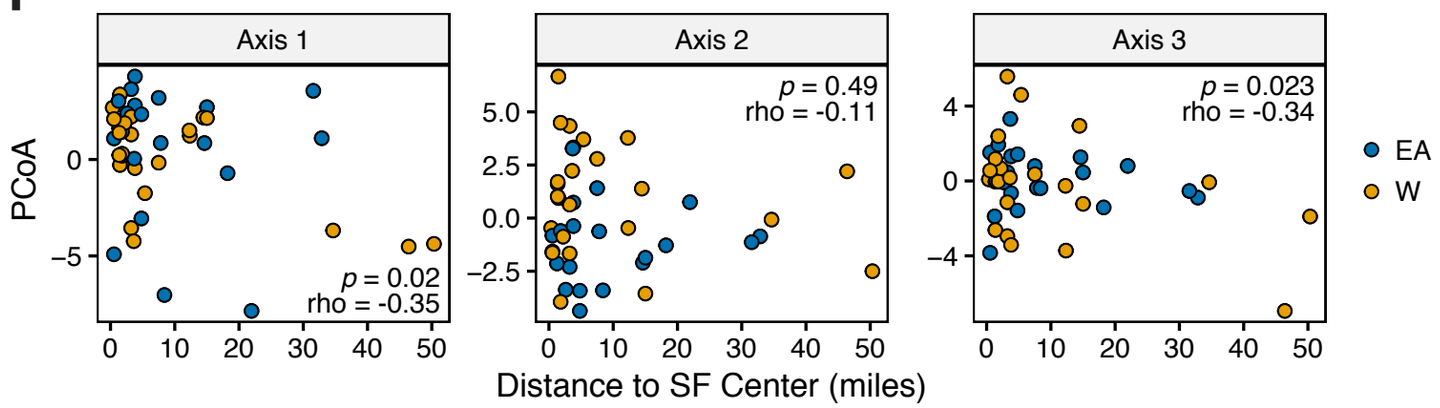
Axis 1
p = 0.02
rho = -0.35
Axis 2
p = 0.49
rho = -0.11
Axis 3
p = 0.023
rho = -0.34
PCoA
Distance to SF Center (miles)
EA
W

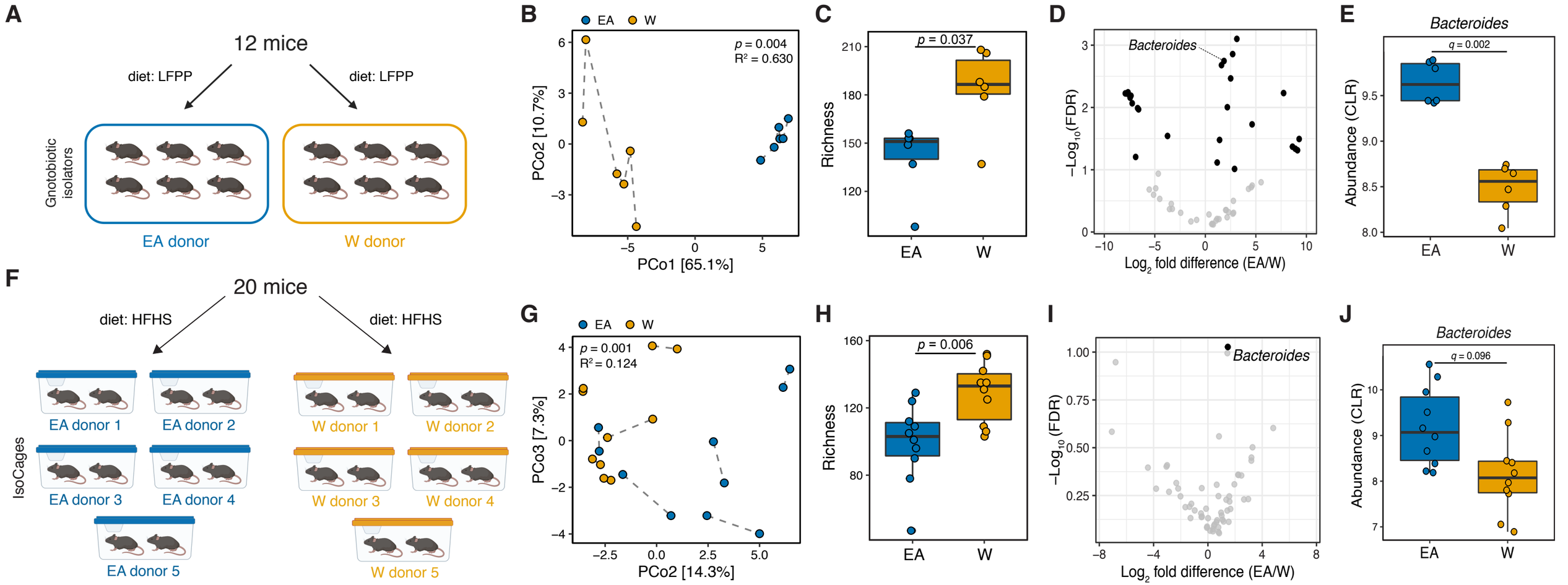
A
12 mice
diet: LFPP
diet: LFPP
Gnotobiotic isolators
EA donor
W donor
B
EA
W
p = 0.004
R² = 0.630
PCo2 [10.7%]
PCo1 [65.1%]
C
p = 0.037
Richness
EA
W
D
Bacteroides
−Log10(FDR)
Log2 fold difference (EA/W)
E
Bacteroides
q = 0.002
Abundance (CLR)
EA
W
F
20 mice
diet: HFHS
diet: HFHS
IsoCages
EA donor 1
EA donor 2
EA donor 3
EA donor 4
EA donor 5
W donor 1
W donor 2
W donor 3
W donor 4
W donor 5
G
EA
W
p = 0.001
R² = 0.124
PCo3 [7.3%]
PCo2 [14.3%]
H
p = 0.006
Richness
EA
W
I
Bacteroides
−Log10(FDR)
Log2 fold difference (EA/W)
J
Bacteroides
q = 0.096
Abundance (CLR)
EA
W

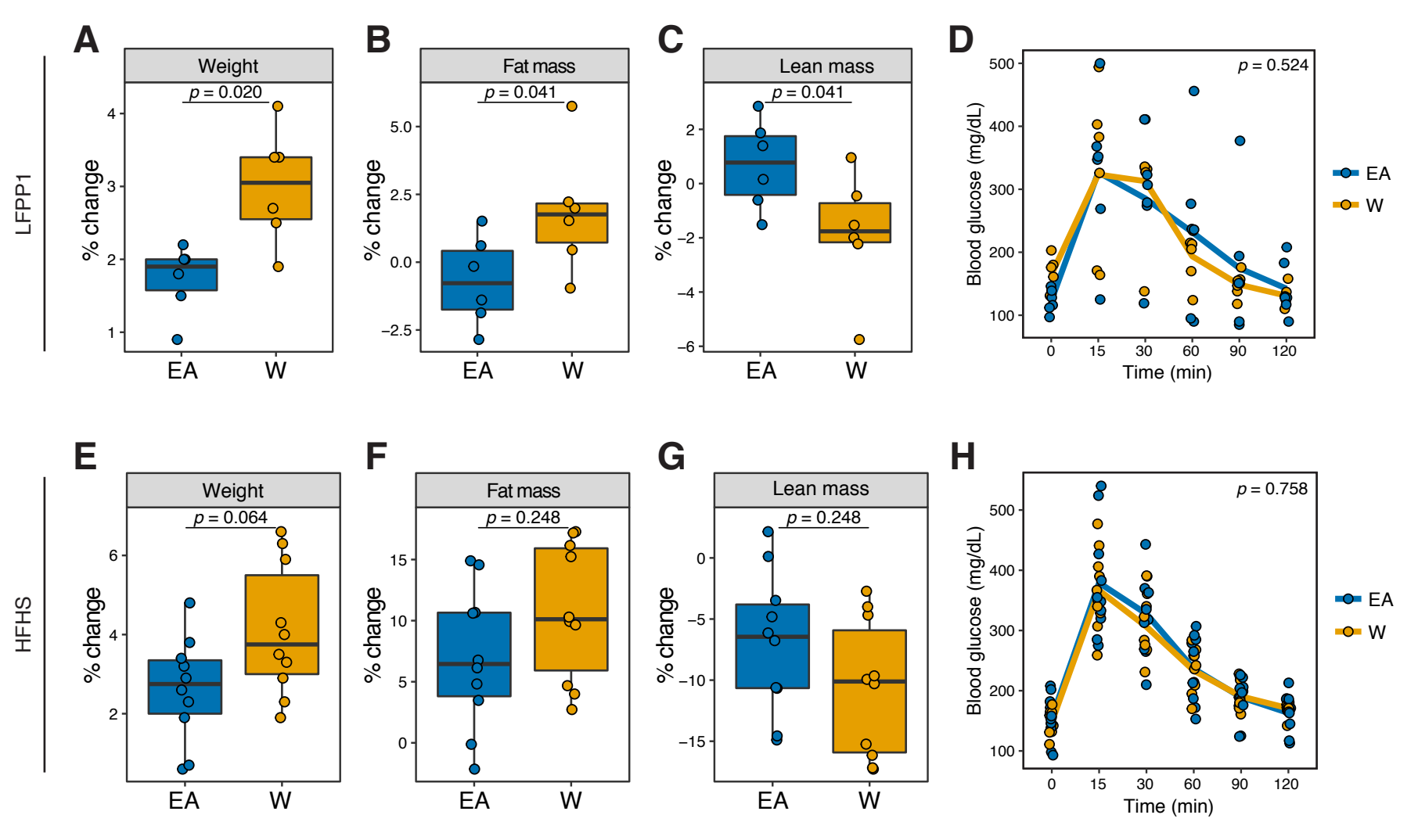
LFPP1
HFHS
A
Weight
p = 0.020
% change
EA
W
B
Fat mass
p = 0.041
% change
EA
W
C
Lean mass
p = 0.041
% change
EA
W
D
p = 0.524
Blood glucose (mg/dL)
Time (min)
EA
W
E
Weight
p = 0.064
% change
EA
W
F
Fat mass
p = 0.248
% change
EA
W
G
Lean mass
p = 0.248
% change
EA
W
H
p = 0.758
Blood glucose (mg/dL)
Time (min)
EA
W

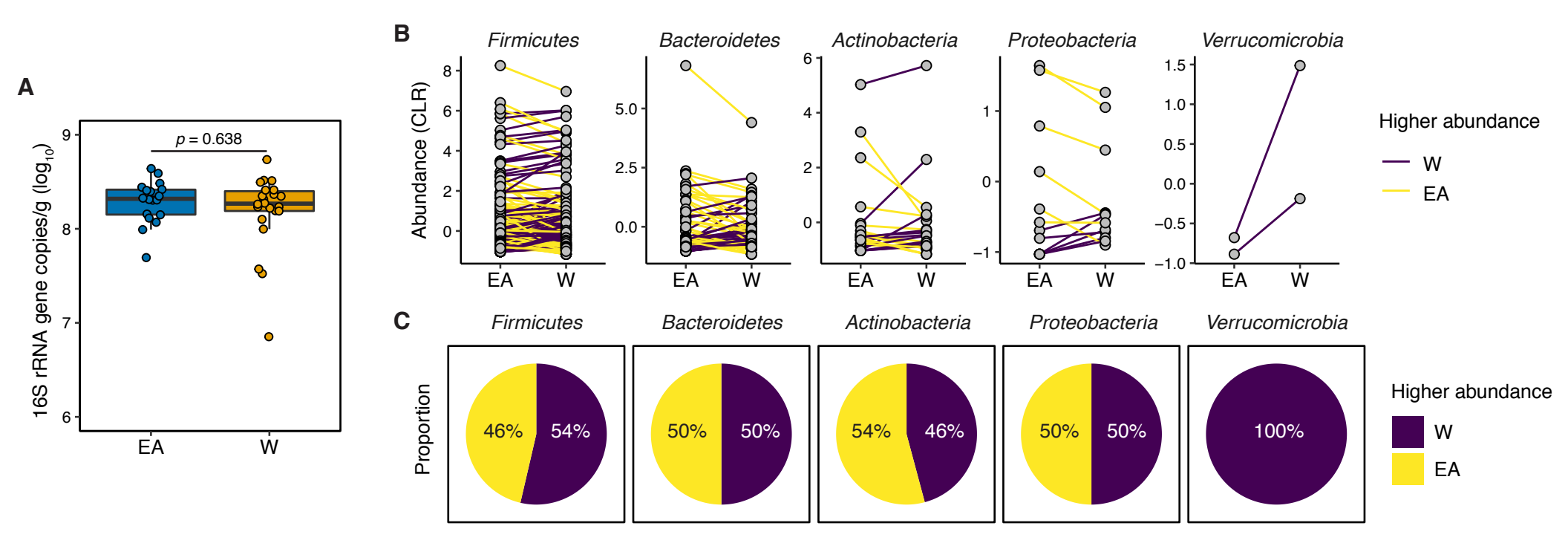
A
16S rRNA gene copies/g (log10)
p = 0.638
EA
W
B
Abundance (CLR)
Firmicutes
Bacteroidetes
Actinobacteria
Proteobacteria
Verrucomicrobia
EA
W
Higher abundance
W
EA
C
Proportion
Firmicutes
Bacteroidetes
Actinobacteria
Proteobacteria
Verrucomicrobia
46%
54%
50%
50%
54%
46%
50%
50%
100%
Higher abundance
W
EA

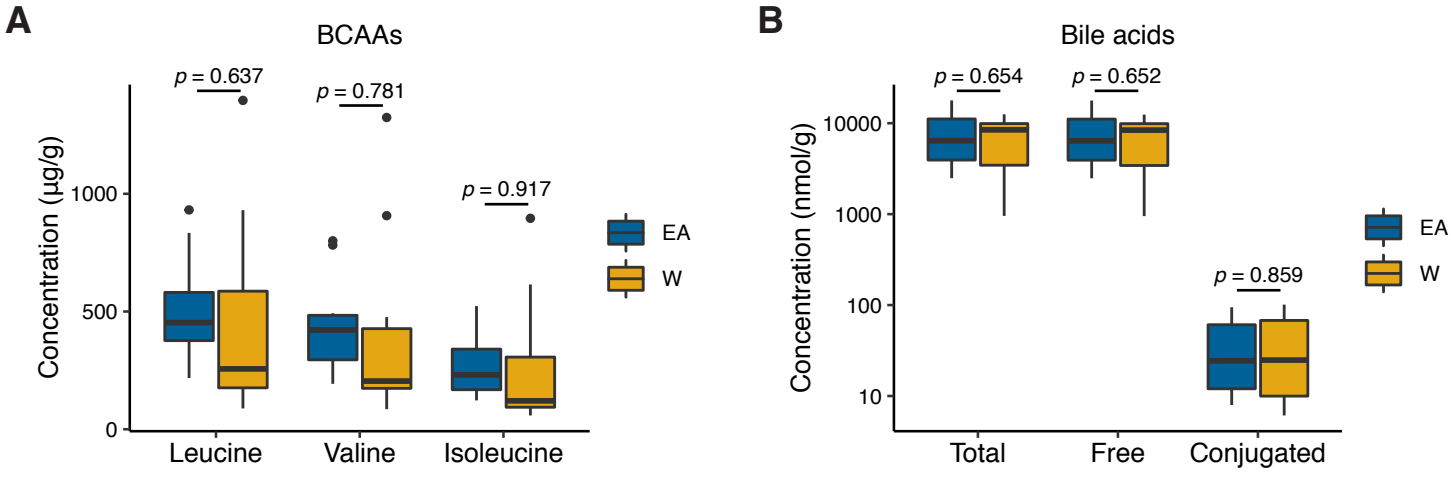
A
BCAAs
p = 0.637
p = 0.781
p = 0.917
Concentration (μg/g)
1000
500
0
Leucine
Valine
Isoleucine
EA
W
B
Bile acids
p = 0.654
p = 0.652
p = 0.859
Concentration (nmol/g)
10000
1000
100
10
Total
Free
Conjugated
EA
W

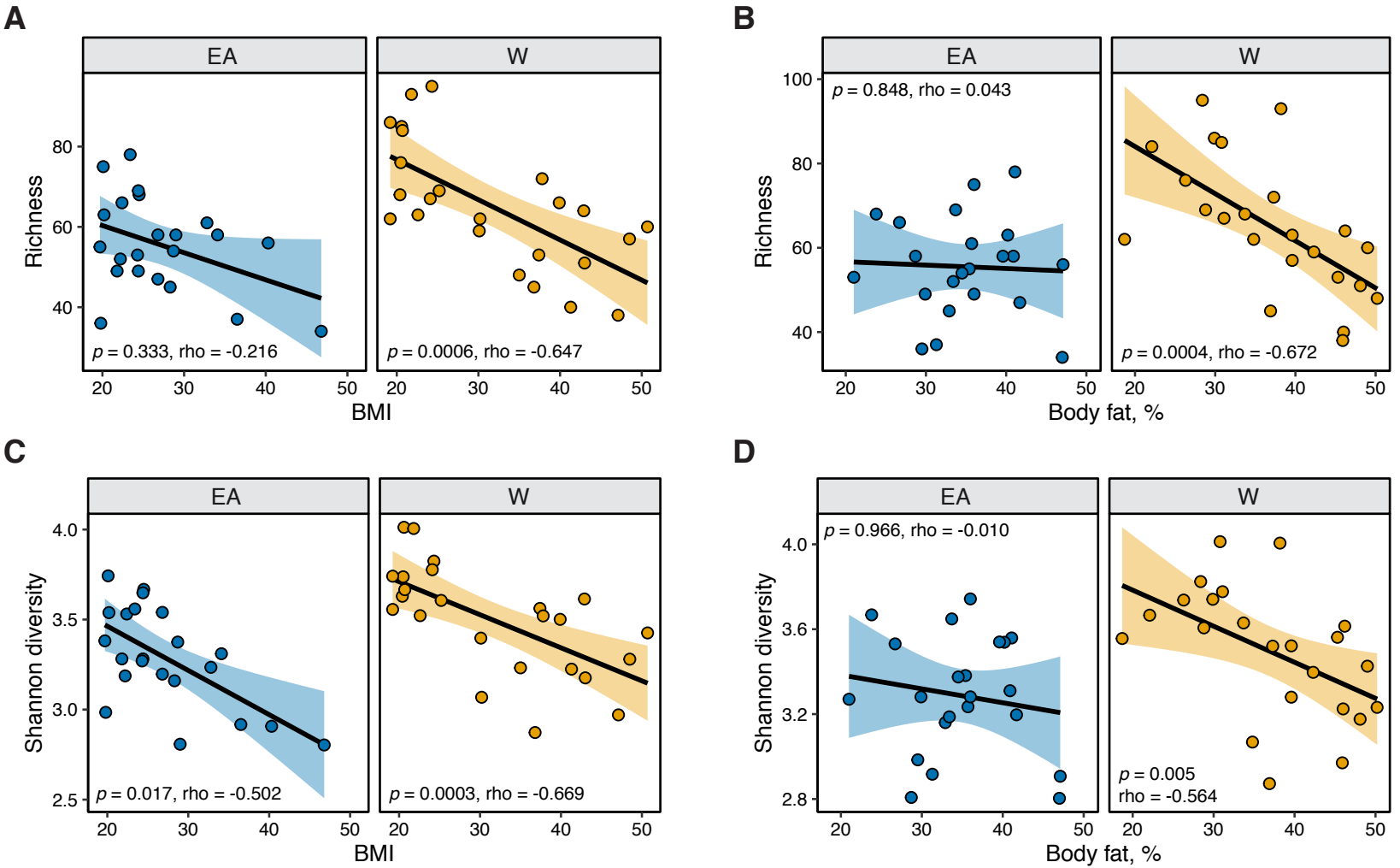
A
EA
W
Richness
BMI
p = 0.333, rho = -0.216
p = 0.0006, rho = -0.647
B
p = 0.848, rho = 0.043
p = 0.0004, rho = -0.672
Body fat, %
C
Shannon diversity
p = 0.017, rho = -0.502
p = 0.0003, rho = -0.669
D
p = 0.966, rho = -0.010
p = 0.005
rho = -0.564

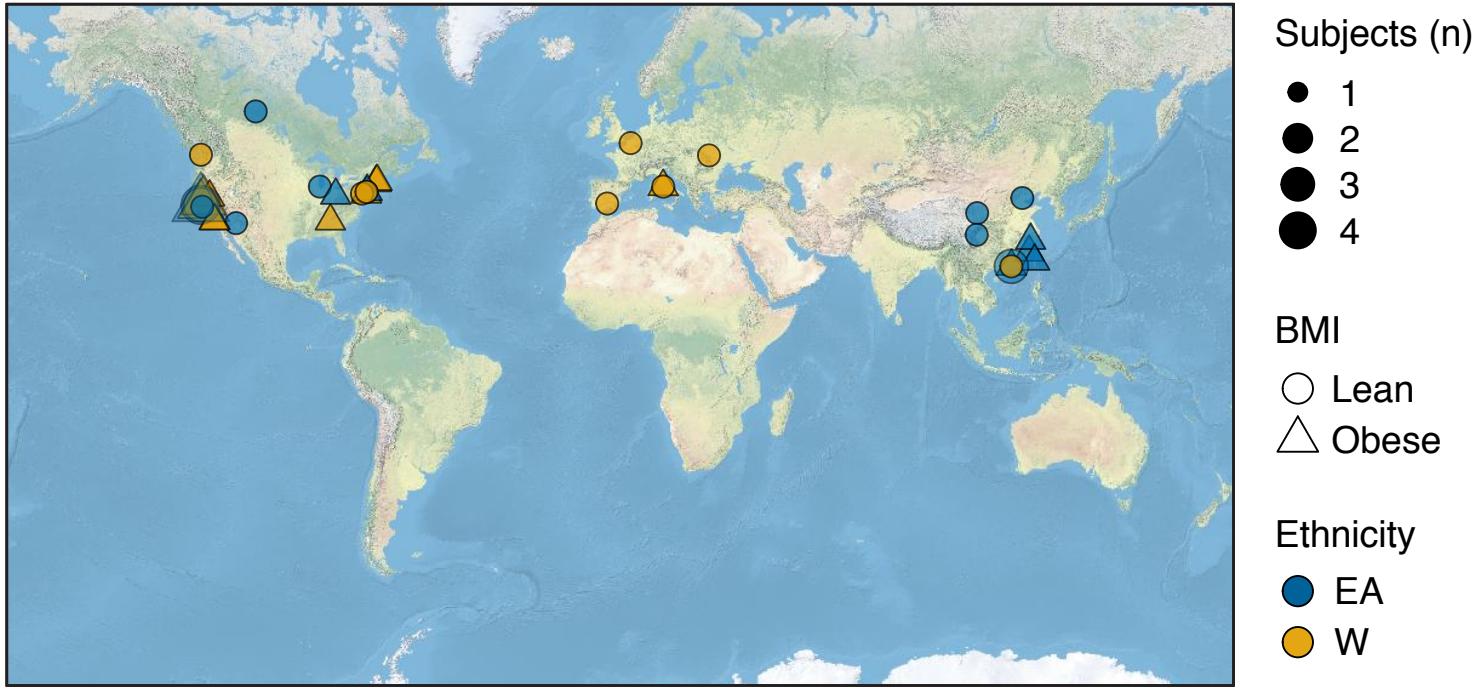
Subjects (n)
1
2
3
4
BMI
Lean
Obese
Ethnicity
EA
W

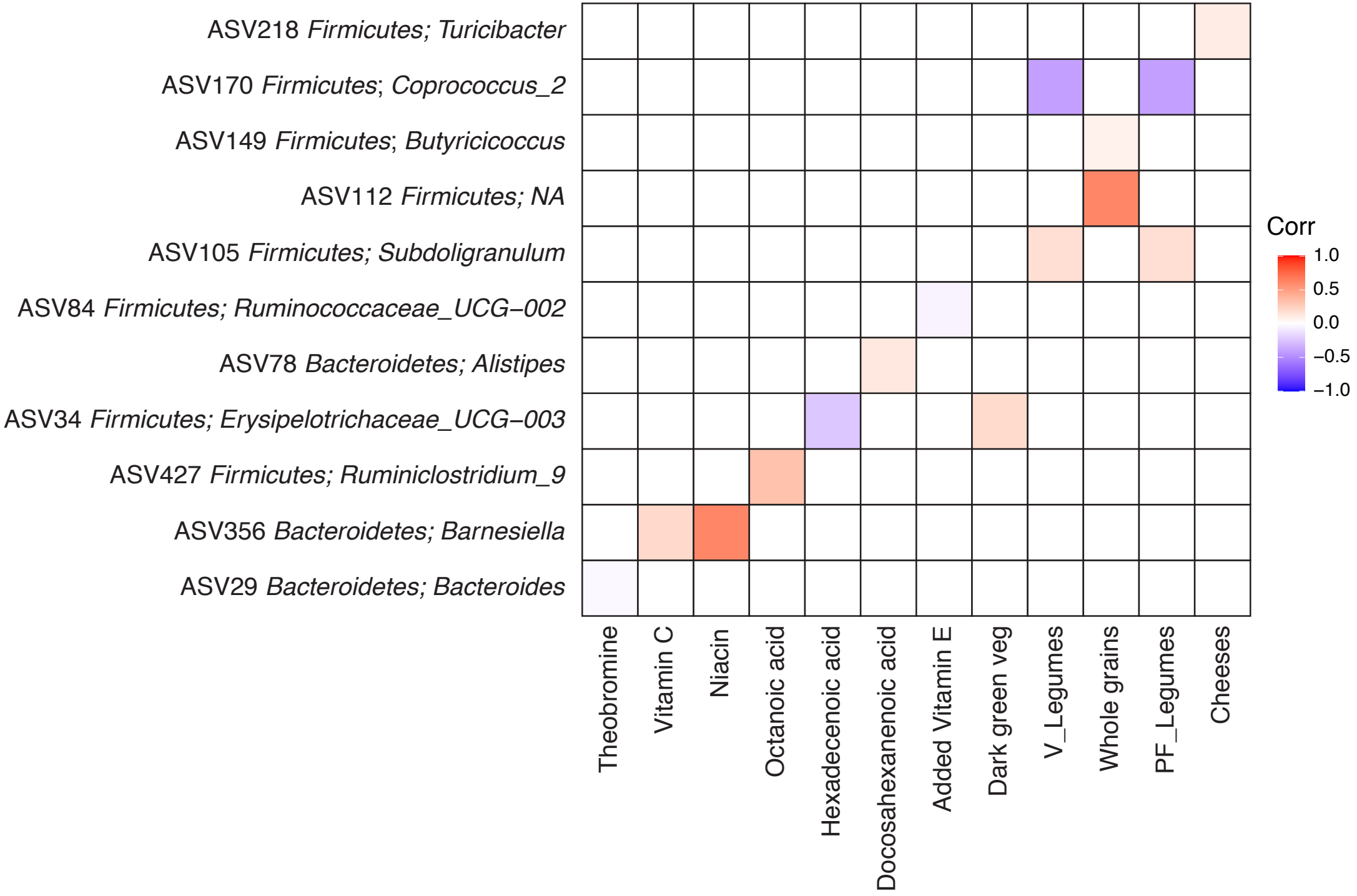
ASV218 Firmicutes; Turicibacter
ASV170 Firmicutes; Coprococcus_2
ASV149 Firmicutes; Butyricicoccus
ASV112 Firmicutes; NA
ASV105 Firmicutes; Subdoligranulum
ASV84 Firmicutes; Ruminococcaceae_UCG–002
ASV78 Bacteroidetes; Alistipes
ASV34 Firmicutes; Erysipelotrichaceae_UCG–003
ASV427 Firmicutes; Ruminiclostridium_9
ASV356 Bacteroidetes; Barnesiella
ASV29 Bacteroidetes; Bacteroides
Theobromine
Vitamin C
Niacin
Octanoic acid
Hexadecenoic acid
Docosahexanenoic acid
Added Vitamin E
Dark green veg
V_Legumes
Whole grains
PF_Legumes
Cheeses
Corr
1.0
0.5
0.0
−0.5
−1.0

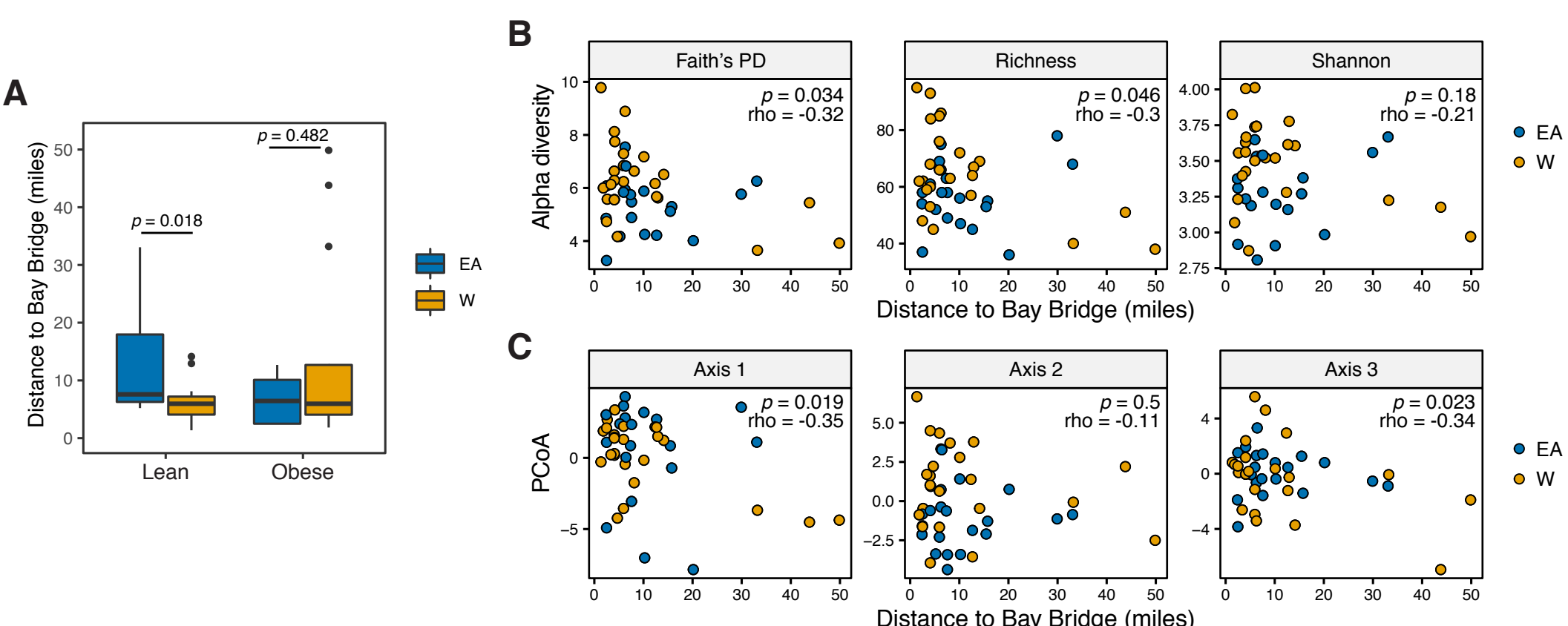
A
Distance to Bay Bridge (miles)
p = 0.482
p = 0.018
Lean
Obese
EA
W
B
Alpha diversity
Faith's PD
p = 0.034
rho = -0.32
Richness
p = 0.046
rho = -0.3
Shannon
p = 0.18
rho = -0.21
Distance to Bay Bridge (miles)
C
PCoA
Axis 1
p = 0.019
rho = -0.35
Axis 2
p = 0.5
rho = -0.11
Axis 3
p = 0.023
rho = -0.34
Distance to Bay Bridge (miles)

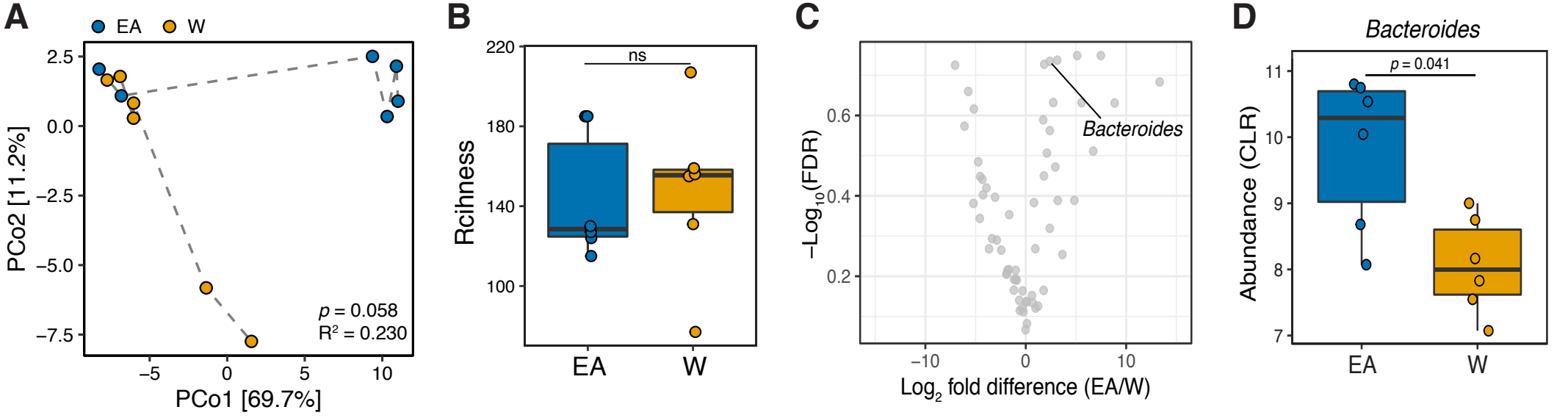
A
EA
W
2.5
0.0
−2.5
−5.0
−7.5
PCo2 [11.2%]
−5
0
5
10
PCo1 [69.7%]
p = 0.058
R² = 0.230
B
220
180
140
100
Rcihness
ns
EA
W
C
0.6
0.4
0.2
−Log10(FDR)
Bacteroides
−10
0
10
Log2 fold difference (EA/W)
D
Bacteroides
p = 0.041
11
10
9
8
7
Abundance (CLR)
EA
W

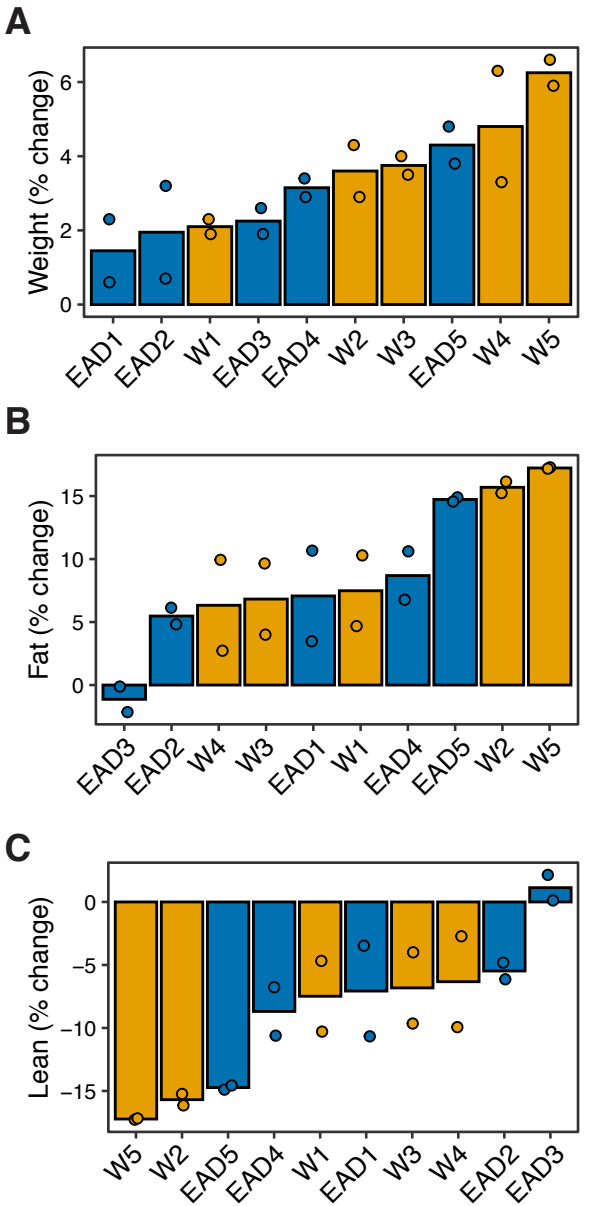
A
Weight (% change)
6
4
2
0
EAD1
EAD2
W1
EAD3
EAD4
W2
W3
EAD5
W4
W5
B
Fat (% change)
15
10
5
0
EAD3
EAD2
W4
W3
EAD1
W1
EAD4
EAD5
W2
W5
C
Lean (% change)
0
−5
−10
−15
W5
W2
EAD5
EAD4
W1
EAD1
W3
W4
EAD2
EAD3